



HAL
open science

Temporo-basal sulcal connections: a manual annotation protocol and an investigation of sexual dimorphism and heritability

Kevin de Matos, Claire Cury, Lydia Chougar, Lachlan T Strike, Thibault Rolland, Maximilien Riche, Lisa Hemforth, Alexandre Martin, Tobias Banaschewski, Arun L W Bokde, et al.

► To cite this version:

Kevin de Matos, Claire Cury, Lydia Chougar, Lachlan T Strike, Thibault Rolland, et al.. Temporo-basal sulcal connections: a manual annotation protocol and an investigation of sexual dimorphism and heritability. *Brain Structure and Function*, 2023, 228 (6), pp.1459-1478. 10.1007/s00429-023-02663-6 . hal-04132176

HAL Id: hal-04132176

<https://hal.science/hal-04132176>

Submitted on 18 Jun 2023

HAL is a multi-disciplinary open access archive for the deposit and dissemination of scientific research documents, whether they are published or not. The documents may come from teaching and research institutions in France or abroad, or from public or private research centers.

L'archive ouverte pluridisciplinaire **HAL**, est destinée au dépôt et à la diffusion de documents scientifiques de niveau recherche, publiés ou non, émanant des établissements d'enseignement et de recherche français ou étrangers, des laboratoires publics ou privés.



Distributed under a Creative Commons Attribution 4.0 International License

Temporo-basal sulcal connections: a manual annotation protocol and an investigation of sexual dimorphism and heritability

Kevin de Matos^{1,2}; Claire Cury³; Lydia Chougar^{1,4}; Lachlan T. Strike^{5,6}; Thibault Rolland¹; Maximilien Riche⁷; Lisa Hemforth¹; Alexandre Martin^{1,8}; Tobias Banaschewski⁹; Arun L.W. Bokde¹⁰; Sylvane Desrivieres¹¹; Herta Flor^{12,13}; Antoine Grigis¹⁴; Hugh Garavan¹⁵; Penny Gowland¹⁶; Andreas Heinz¹⁷; Rüdiger Brühl¹⁸; Jean-Luc Martinot¹⁹; Marie-Laure Paillère Martinot²⁰; Eric Artiges²¹; Frauke Nees^{9,12,30}; Dimitri Papadopoulos Orfanos¹⁴; Herve Lemaitre^{14,22}; Tomáš Paus^{23,24}; Luise Poustka²⁵; Sarah Hohmann⁹; Sabina Millenet⁹; Juliane H. Fröhner²⁶; Michael N. Smolka²⁶; Nilakshi Vaidya²⁷; Henrik Walter¹⁷; Robert Whelan²⁸; Gunter Schumann^{27, 29}; Vincent Frouin¹⁴; IMAGEN Consortium; Meritxell Bach Cuadra²; Olivier Colliot¹; Baptiste Couvy-Duchesne^{1,31*}

ORCID

KdM (Ø); CC (0000-0002-9903-7940); LC (0000-0001-9306-5687); LTS (0000-0003-2885-5898); TR (Ø); MR (Ø); LH (Ø); AM (Ø); TB (0000-0003-4595-1144); ALWB (0000-0003-0114-4914); SD (0000-0002-9120-7060); HF (0000-0003-4809-5398); AG (Ø); HG (0000-0002-8939-1014); PG (0000-0002-4900-4817); AH (0000-0001-5405-9065); RB (0000-0003-0111-5996); JLM (0000-0002-0136-0388); MLPM (0000-0002-0452-2450); EA (0000-0003-4461-7646); FN (0000-0002-7796-8234); DPO (0000-0002-1242-8990); HL (0000-0002-5952-076X); TP (0000-0003-1495-9338); LP (0000-0002-7738-4394); SH (0000-0002-5175-6698); SM (0000-0002-8882-2740); JHF (0000-0002-8493-6396); MNS (0000-0001-5398-5569); NV (0000-0002-4600-7158); HW (0000-0002-9403-6121); RW (0000-0002-2790-7281); GS (0000-0003-4905-5523); VF (0000-0001-9360-6623); MBC (0000-0003-2730-4285); OC (0000-0002-9836-654X); BCD (0000-0002-0719-9302)

¹ Sorbonne Université, Institut du Cerveau - Paris Brain Institute - ICM, CNRS, Inria, Inserm, AP-HP, Hôpital de la Pitié Salpêtrière, F-75013, Paris, France

² CIBM Center for Biomedical Imaging, Switzerland; Radiology Department, Lausanne University and University Hospital, Switzerland

³ University of Rennes, CNRS, Inria, Inserm, IRISA UMR 6074, Empenn ERL U-1228, F-35000 Rennes, France

⁴ Service de neuroradiologie, AP-HP, Pitié-Salpêtrière, Paris, France

⁵ The University of Queensland, Queensland Brain Institute, Qld 4072, Australia

⁶ Psychiatric Genetics, QIMR Berghofer Medical Research Institute, Brisbane, Australia

⁷ Sorbonne University, Department of Neurosurgery, AP-HP, La Pitié-Salpêtrière Hospital, F-75013, Paris, France

⁸ Inria Sophia Antipolis, Morpheme Project, France

⁹ Department of Child and Adolescent Psychiatry and Psychotherapy, Central Institute of Mental Health, Medical Faculty Mannheim, Heidelberg University, Square J5, 68159 Mannheim, Germany

¹⁰ Discipline of Psychiatry, School of Medicine and Trinity College Institute of Neuroscience, Trinity College Dublin, Dublin, Ireland

¹¹ Centre for Population Neuroscience and Precision Medicine (PONS), Institute of Psychiatry, Psychology & Neuroscience, SGDP Centre, King's College London, United Kingdom

¹² Institute of Cognitive and Clinical Neuroscience, Central Institute of Mental Health, Medical Faculty Mannheim, Heidelberg University, Square J5, Mannheim, Germany

¹³ Department of Psychology, School of Social Sciences, University of Mannheim, 68131 Mannheim, Germany

¹⁴ NeuroSpin, CEA, Université Paris-Saclay, F-91191 Gif-sur-Yvette, France

¹⁵ Departments of Psychiatry and Psychology, University of Vermont, 05405 Burlington, Vermont, USA

¹⁶ Sir Peter Mansfield Imaging Centre School of Physics and Astronomy, University of Nottingham, University Park, Nottingham, United Kingdom

¹⁷ Department of Psychiatry and Psychotherapy CCM, Charité – Universitätsmedizin Berlin, corporate member of Freie Universität Berlin, Humboldt-Universität zu Berlin, and Berlin Institute of Health, Berlin, Germany

¹⁸ Physikalisch-Technische Bundesanstalt (PTB), Braunschweig and Berlin, Germany

¹⁹ Institut National de la Santé et de la Recherche Médicale, INSERM U 1299 "Trajectoires développementales & psychiatrie", University Paris-Saclay, CNRS; Ecole Normale Supérieure Paris-Saclay, Centre Borelli; Gif-sur-Yvette, France

²⁰ Institut National de la Santé et de la Recherche Médicale, INSERM U 1299 "Trajectoires développementales & psychiatrie", University Paris-Saclay, CNRS; Ecole Normale Supérieure Paris-Saclay, Centre Borelli; Gif-sur-Yvette; and AP-HP. Sorbonne University, Department of Child and Adolescent Psychiatry, Pitié-Salpêtrière Hospital, Paris; France

²¹ Institut National de la Santé et de la Recherche Médicale, INSERM U 1299 "Trajectoires développementales & psychiatrie", University Paris-Saclay, CNRS; Ecole Normale Supérieure Paris-Saclay, Centre Borelli; Gif-sur-Yvette; and Psychiatry Department, EPS Barthélémy Durand, Etampes; France

²² Institut des Maladies Neurodégénératives, UMR 5293, CNRS, CEA, Université de Bordeaux, 33076 Bordeaux, France

²³ Departments of Psychiatry and Neuroscience, Université de Montréal and Centre Hospitalier Universitaire Sainte-Justine, Montréal, Québec, Canada

²⁴ Departments of Psychiatry and Psychology, University of Toronto, Toronto, Ontario, Canada

²⁵ Department of Child and Adolescent Psychiatry and Psychotherapy, University Medical Centre Göttingen, von-Siebold-Str. 5, 37075, Göttingen, Germany

²⁶ Department of Psychiatry and Neuroimaging Center, Technische Universität Dresden, Dresden, Germany

²⁷ Centre for Population Neuroscience and Stratified Medicine (PONS), Department of Psychiatry and Neuroscience, Charité Universitätsmedizin Berlin, Germany

²⁸ School of Psychology and Global Brain Health Institute, Trinity College Dublin, Ireland

²⁹ Centre for Population Neuroscience and Precision Medicine (PONS), Institute for Science and Technology of Brain-inspired Intelligence (ISTBI), Fudan University, Shanghai, China

³⁰ Institute of Medical Psychology and Medical Sociology, University Medical Center Schleswig Holstein, Kiel University, Kiel, Germany

³¹ Institute for Molecular Biosciences, the University of Queensland, 4062 St Lucia, Queensland

* Corresponding author:

Baptiste Couvy-Duchesne, ICM – Paris Brain Institute

ARAMIS team

Pitié-Salpêtrière Hospital

47-83, boulevard de l'Hôpital, 75651 Paris Cedex 13, France

E-mail: baptiste.couvy@icm-institute.org

Abstract

The temporo-basal region of the human brain is composed of the collateral, the occipito-temporal, and the rhinal sulci.

We manually rated (using a novel protocol) the connections between rhinal/collateral (RS-CS), collateral/occipito-temporal (CS-OTS) and rhinal/occipito-temporal (RS-OTS) sulci, using the MRI of nearly 3,400 individuals including around 1000 twins. We reported both the associations between sulcal polymorphisms as well with a wide range of demographics (e.g. age, sex, handedness). Finally, we also estimated the heritability, and the genetic correlation between sulcal connections.

We reported the frequency of the sulcal connections in the general population, which were hemisphere dependent. We found a sexual dimorphism of the connections, especially marked in the right hemisphere, with a CS-OTS connection more frequent in females (approximately 35-40% versus 20-25% in males) and an RS-CS connection more common in males (approximately 40-45% versus 25-30% in females). We confirmed associations between sulcal connections and characteristics of incomplete hippocampal inversion (IHI).

We estimated the broad sense heritability to be 0.28-0.45 for RS-CS and CS-OTS connections, with hints of dominant contribution for the RS-CS connection. The connections appeared to share some of their genetic causing factors as indicated by strong genetic correlations. Heritability appeared much smaller for the (rarer) RS-OTS connection.

Keywords

Sulcal variability; Temporal lobe; Rhinal sulcus; Collateral sulcus; Occipito-temporal sulcus; Twin heritability

Highlights

- We introduced a protocol for classification of temporo-basal sulcal connections.
- Frequency of sulcal connections differed between the two hemispheres and between sex.
- We found moderate broad-sense heritability for two of the connections.
- Sulcal connections shared genetic and environmental causal factors.

1. Introduction

During fetal development of the human cerebral cortex, in the second trimester of pregnancy, the initially smooth cortex starts growing into multiple folds. This process, called gyrification, produces multiple sulci on the surface of the brain (Chi, Dooling, et Gilles 1977; Zilles et al. 1988). Individuals largely share the same set of sulci that present high inter-individual variability in terms of shape, length and sulcal connections, whose origin is not well-known (Ronan et Fletcher 2015; Borrell 2018; Kroenke et Bayly 2018).

From a genetic point of view, many studies have highlighted the possible genetic influences on the sulcal structure. The study by Pizzagalli et al. (2020) concluded that sulcal width was the most heritable measure (comparing variations in the length, depth, width, and surface area of several sulci associated with certain diseases). The authors also showed earlier forming sulci exhibited higher heritability (on average, for all four measurements) and that each hemisphere had partly specific genetic influences. The study by Yang et al. (2020), based on young Chinese adults, identified significant sex differences in sulcal morphology in several brain regions. In addition, monozygotic twins have been shown to have more similar sulcal patterns (sulcal depth, overall brain shape, study of geometric features by graph matching approach) than unrelated individuals (Lohmann 1999; Mohr et al. 2004; Im et al. 2011), which suggests a genetic contribution. Nevertheless, the study by Troiani et al. (2022) targeting the variability of the orbital sulci and using monozygotic and dizygotic twins showed that their variability was not of genetic origin, suggesting the complexity of being able to generalize findings across the whole brain.

From a clinical point of view, numerous studies have highlighted associations between sulcal morphology and various pathologies. The study by Kippenhan et al. (2005) showed a reduction in the depth of certain sulci (particularly the collateral sulcus) in patients with Williams syndrome. Other pathologies such as Down syndrome (Yun et al. 2021) autism (Nordahl et al. 2007; Auzias et al. 2014; Ecker et al. 2016; Libero et al. 2019), dyslexia (Im et

al. 2016), bipolar disorder and unipolar depression (Penttilä et al. 2009), schizophrenia (Cachia et al. 2008; Penttilä et al. 2008), Parkinson's disease (Pereira et al. 2012) or Alzheimer's disease (Im et al. 2008) have shown associations with certain sulcal morphologies (sulcal depth, surface-based morphometry, local gyrification index, etc.).

Connection-based sulcal variations are mainly studied by neurosurgeons, especially in the medio-basal part of the temporal lobe, which is a path of surgical approach used to treat pathologies such as some tumors and arteriovenous malformations, or pharmaco-resistant temporal lobe epilepsy (Cikla et al. 2016; Ovalioglu et al. 2018). Several *post mortem* studies have focused on describing the sulci of the inferior surface of the temporal lobe (collateral, occipito-temporal, and rhinal), by measuring their length, depth and mutual connections using dissected brains (Cikla et al. 2016; Ovalioglu et al. 2018). Another study (Kim et al. 2008), using MRI images, showed a possible link between temporal lobe epilepsy and the mutual connections of these sulci. In these three studies, each time a limited number of individuals was studied ($N < 100$) and the classifications used were not strictly similar (the meaning of what a “connection” is varies), producing results difficult to generalise and compare between them.

Here, we focused on the connections between sulci of the medio-basal part of the temporal lobe, namely the rhinal (RS), collateral (CS) and occipito-temporal (OTS) sulci. We selected the medio-basal temporal lobe because these connections have been understudied (small studies, inconsistent protocols and results) and they may relate to incomplete hippocampal inversion (IHI), a phenotype of interest due to its possible association with epilepsy (Bajic et al. 2009). The association between the abnormal positioning of the hippocampus and the depth of the collateral sulcus has been described in several studies (Baulac et al. 1998; Bernasconi et al. 2005; Cury et al. 2015) but the link between the sulcal depths and connections between these three sulci has not yet been established.

We aimed to study sulci connections using MRI images from large population samples, in order to produce robust results about sulcal connections frequencies, and associations with

demographics and IHI. In addition, we used twins to estimate the extent to which individual differences can be explained by genetics (heritability) and environmental contributions. Finally, we also reported the co-occurrence of sulcal connections, which indicates whether similar genetic or environmental factors contribute to local or global sulcal polymorphism. In absence of an established manual protocol for large datasets and due to the complexity of automating this task, we relied on manual rating of sulcal connections and we created a modular rating protocol, which may be easily extended to other sulci. Indeed, sulcal connections are not easily extracted using automated image processing algorithms unlike sulcal depths. Our protocol and approach ensure that the data generated in this study will be compatible with future extended descriptions of sulcal connections that may focus on complementary brain regions.

Our starting hypothesis is that there is a stable frequency of sulcal connections that can be observed across independent samples of healthy subjects. This precise frequency of sulcal connections is yet unclear as previous studies relied on a limited number of individuals inducing very wide confidence intervals (**Table S4**). The second hypothesis is that of a heritable component to these sulcal connections, in line with the genetic influence that have been reported for sulcal characteristics such as length, depth or width (Pizzagalli et al. 2020). Lastly, our investigation of associations between sulcal connection and demographics or IHI is largely exploratory, and we do not have specific hypotheses about the possible associations.

2. Materials and Methods

2.1 Participants

We studied three databases: IMAGEN, QTIM, and QTAB. We kept only the MRIs whose quality made it possible to clearly see the sulci of interest (visual exclusion during subjects rating). The multi-centric European database IMAGEN (the IMAGEN consortium et al. 2010) contains data collected in 2,089 young individuals from four European countries (France, Germany, United Kingdom, and Ireland). We used the MRI images and demographic information acquired at baseline, when participants were 14 years old. The MRIs of 2,005 individuals were judged of sufficient quality for sulci assessment. The Queensland Twin IMaging (QTIM) database (de Zubicaray et al. 2008; Strike, Blokland, et al. 2022) contains data collected in over 1000 Australian individuals between 18 and 30 years of age. The MRIs of 979 individuals were judged of sufficient quality, which consisted of 144 complete monozygotic (MZ) pairs, 180 complete dizygotic (DZ) pairs, and 331 single members of a twin pair and siblings of twins. Finally, The Queensland Twin Adolescent Brain (QTAB) sample (Strike, Hansell, Chuang, et al. 2022; Strike, Hansell, Miller, et al. 2022) contains 422 Australian twins aged from 9 to 14 years. MRIs of 405 individuals were judged of sufficient quality, which comprised 101 complete monozygotic twin pairs, 94 complete dizygotic pairs and 15 unrelated individuals. We summarised the sample demographics in **Table 1**.

2.1.1 Patient consent statement and ethics approval

IMAGEN was approved by the local ethic committees and a detailed description of recruitment, assessment procedures, and exclusion/inclusion criteria have been published in (the IMAGEN consortium et al. 2010), QTIM was approved by the Human Research Ethics Committees (HREC) at the University of Queensland (de Zubicaray et al. 2008), and QTAB was approved

by the Children's Health Queensland HREC and the University of Queensland HREC (Strike, Hansell, Chuang, et al. 2022).

Table 1. Characteristics of the studied population

	IMAGEN	QTIM	QTAB	QTIM+QTAB
N	2,005	979	405	1,384
Age (years): mean \pm SD	14.6 \pm 0.4	22.9 \pm 2.8	11.3 \pm 1.4	19.5 \pm 5.8
Age (years): range	12.9 - 17.2	18.1 - 30.1	9.0 - 14.4	9.0 - 30.1
% Female (N)	51.27 (1,028)	61.9 (606)	48.89 (198)	58.09 (804)
handedness (N): Right / Left / Both / Undefined	1,737 / 218 / 14 / 36	979 / - / - / -	334 / 71 / - / -	1,313 / 71 / - / -
Site (N)	8	1	1	2
Twins (N) complete pairs	-	324	195	519
incl. complete MZ / DZ	-	144 / 180	101 / 94	245 / 274
incl. complete MZMM / MZFF	-	51 / 93	53 / 48	104 / 141
incl. complete DZMM / DZFF	-	33 / 74	25 / 27	58 / 101
incl. complete DZMF + DZFM	-	73	42	115

SD = Standard-Deviation; MZ = Monozygotic; DZ = Dizygotic; MZMM / MZFF = Monozygotic Male / Female; DZMM / DZFF = Dizygotic Male / Female; DZMF + DZFM = Dizygotic Male + Female

2.2 MRI Acquisition

We relied on 3-Dimensional T1-weighted anatomical MRI, to determine the connections between sulci.

For IMAGEN, the MRIs were acquired on a range of 3 Tesla scanners (Siemens Verio and TimTrio, Philips Achieva, General Electric Signa Excite, and Signa HDx), which depended on the acquisition site. All sites used the same acquisition parameters of an MPRAGE (Magnetization Prepared Rapid Acquisition Gradient Echo) sequence (TR=2300ms; TE=2.8ms; flip angle=9°; resolution=1.1×1.1×1.1 mm). In order to assess the sulcal connections with a standardized MRI orientation, the images were registered toward the MNI152 atlas using

the automated affine transformation method FLIRT from FSL software (Jenkinson et Smith 2001; Jenkinson et al. 2002), as in Cury et al.

In QTIM, the MRIs were acquired on a 4 Tesla Bruker Medspec scanner using an inversion recovery rapid gradient echo protocol (TI=700ms; TR=1500ms; TE=3.35ms; flip angle=8°; resolution=0.94×0.98×0.98mm). We registered the MRIs in the MNI152 space using the t1-linear pipeline in Clinica (Wen et al. 2020; Routier et al. 2021).

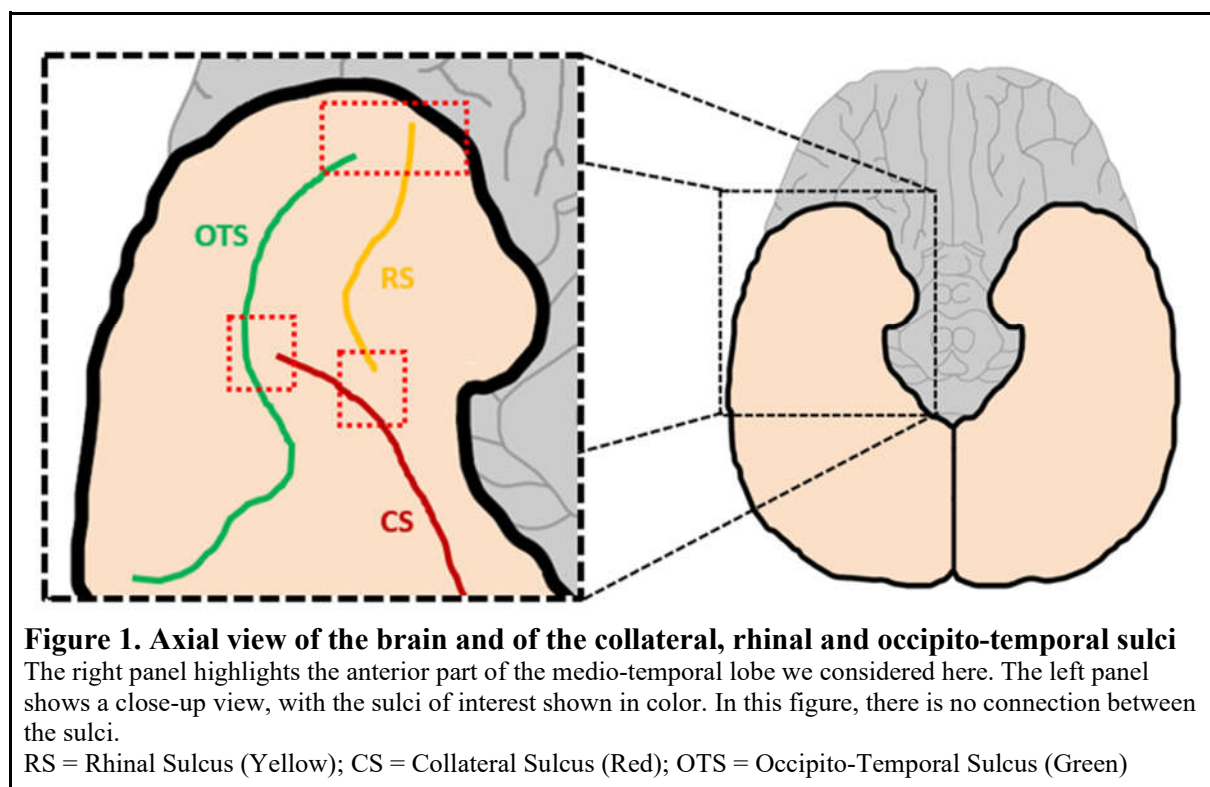
QTAB images were acquired on a 3 Tesla Magnetom Prisma scanner (Siemens Medical Solutions, Erlangen) using a 3D MP2RAGE (Magnetization Prepared 2 Rapid Acquisition Gradient Echoes) sequence (TI=700ms; TR=4000ms; TE=2.99ms; flip angle=6°; resolution=0.8×0.8×0.8mm). As for QTIM, the MRIs were registered in the MNI152 space using the t1-linear pipeline of Clinica.

The differences in acquisition parameters between the three databases did not impact the manual morphological classification. For example, **Figure S1** shows a coronal view from the three databases. Overall, the image resolution can be a limiting factor for manual rating, but the voxel sizes ranged from 0.8×0.8×0.8mm (QTAB) to 1.1×1.1×1.1mm (IMAGEN), which were not visually disturbing to classify the sulcal connections. Note that the image registration in the MNI152 space simplifies the classification as it homogenizes the orientation and position of the brain as well as the resolution of the databases (1x1x1mm). More advanced image processing and harmonization remains warranted (and an active field of research) when extracting automatic structural measurements (Gebre et al. 2023).

2.3 Radiological assessment of medio-temporal lobe sulci: Classification protocol

2.3.1. A connection-based classification

We propose a classification based on the physical connections between the collateral (CS), rhinal (RS) and occipito-temporal (OTS) sulci. To facilitate manual rating, we have only considered connections in the anterior part of the medio-temporal lobes (the posterior part is more variable and more complex to classify) (**Figure 1**). For the same reason, we have not considered the possible morphological sulcal variations (subcomponents, side branches, number of segments, etc.). For example, we have considered the anterior transverse collateral sulcus to be part of the collateral sulcus.



We considered each connection as a binary variable, which makes our classification modular and easy to extend to other sulci. Each variable denotes the presence (coded 1) or absence (coded 0) of connection between the rhinal and collateral sulci (noted RS-CS connection), between the collateral and occipito-temporal sulci (CS-OTS connection) and between the rhinal and occipito-temporal sulci (RS-OTS connection). Our rating considers the

connections individually (connection-based classification). It allows studying specific associations with variables of interest (e.g. demographics, or clinical), but also allows studying the co-occurrence of connections as well as the total number of connections. Previous works relied on pattern-based classification, i.e. patterns comprising several sulci rather than individual connections were rated (Kim et al. 2008; Cikla et al. 2016; Ovalioglu et al. 2018), which does not facilitate the analyses and is more difficult to update when considering additional sulci. Importantly, our connection-based classification may be easily converted into pattern-based classification if needed (see supplementary materials for the correspondence with pattern-based classification).

2.3.2. Collateral sulcus variations and anterior/posterior boundary of the medio-temporal lobe

Although the collateral sulcus (CS) has a very constant morphology in its anterior part, it can be present as a single-branch, separated into two branches (an occipital branch and a temporal branch), or can be composed of two non-connected sulci in its posterior part (**Figure 2**). This sulcus delimits the medial occipito-temporal gyrus (formed by the para/hippocampal gyrus in the anterior part and the lingual gyrus in the posterior part) from the lateral occipitotemporal gyrus, also called the fusiform gyrus (**Figure 2**). We considered the anterior/posterior boundary of the medio-temporal lobe to be located at the split of the CS into two branches or, in absence of a split, around the center of the CS, approximately at the separation of the hippocampal gyrus and the lingual gyrus (**Figure 2**).

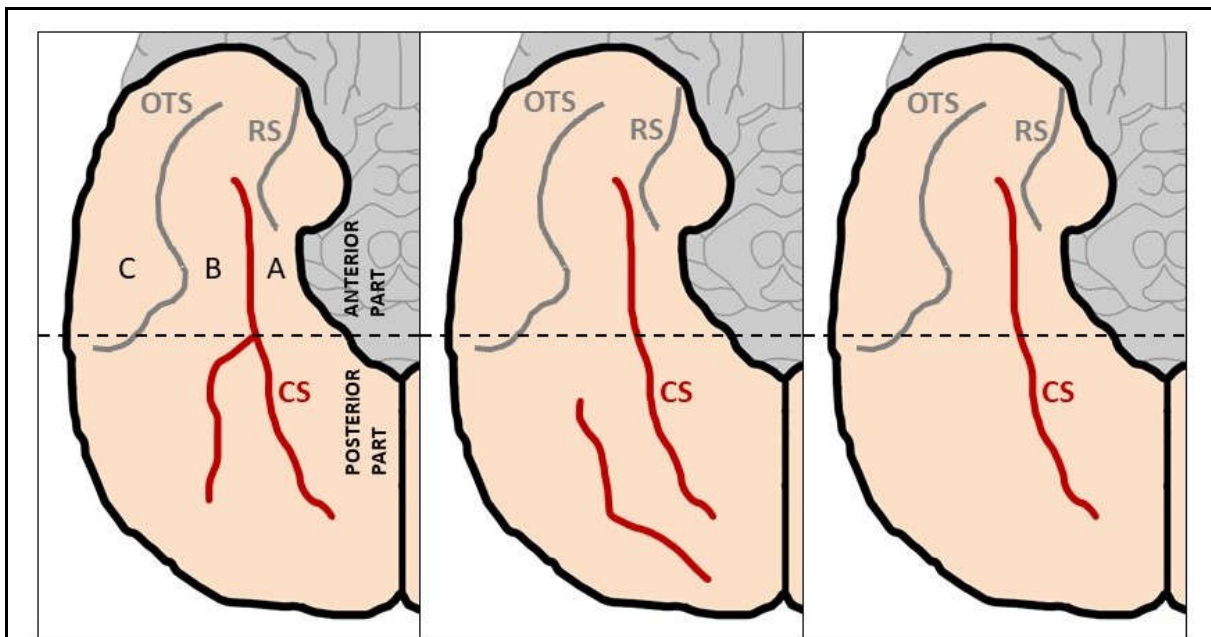


Figure 2. View of collateral sulcus variations and of the anterior/posterior boundary of the medio-temporal lobe

The collateral sulcus is shown in red, and can be separated into two branches posteriorly (left); be composed of two non-connected sulci posteriorly (center); be composed of a single sulcus (right); A = Hippocampal gyrus; B = Fusiform gyrus; C = Inferior temporal gyrus; RS = Rhinal Sulcus (Gray); CS = Collateral Sulcus (Red); OTS = Occipito-Temporal Sulcus (Gray)

2.3.3. Occipito-temporal and Rhinal sulci variations

The occipito-temporal sulcus (OTS) is the sulcus with the most frequent morphological variations among the three sulci considered, with up to six distinct sections recorded (Cikla et al. 2016). It is located laterally to the collateral sulcus. It delimits, medially, the lateral occipitotemporal (fusiform) gyrus and, laterally, the inferior temporal gyrus (**Figure 2**).

The rhinal sulcus (RS) is the least described sulcus of the three in the scientific literature because it has long been considered part of the collateral sulcus (so called “anterior collateral sulcus”) rather than a separate sulcus. It is located in the antero-medial position of the collateral sulcus.

2.3.4. Assessing connections between sulci and visual rating guidelines

We assessed the T1w images with the medInria visualization software (<https://med.inria.fr/>). For each hemisphere, we scrolled through the axial view to distinguish each sulcus with their mutual connections (**Figure 3**). Connection is observed when there is a meeting point at any

depth between two sulci (**Figure 3** - III axial, III coronal and IV axial). For a good appreciation of the connections, we recommend considering both the coronal view and the axial view, although we often found the coronal view to be the most conclusive (**Figure 3**). We recommend starting by locating the collateral sulcus (which has the least morphological variations) and then the other two sulci. Another figure is also available in supplementary materials (**Figure S2**).

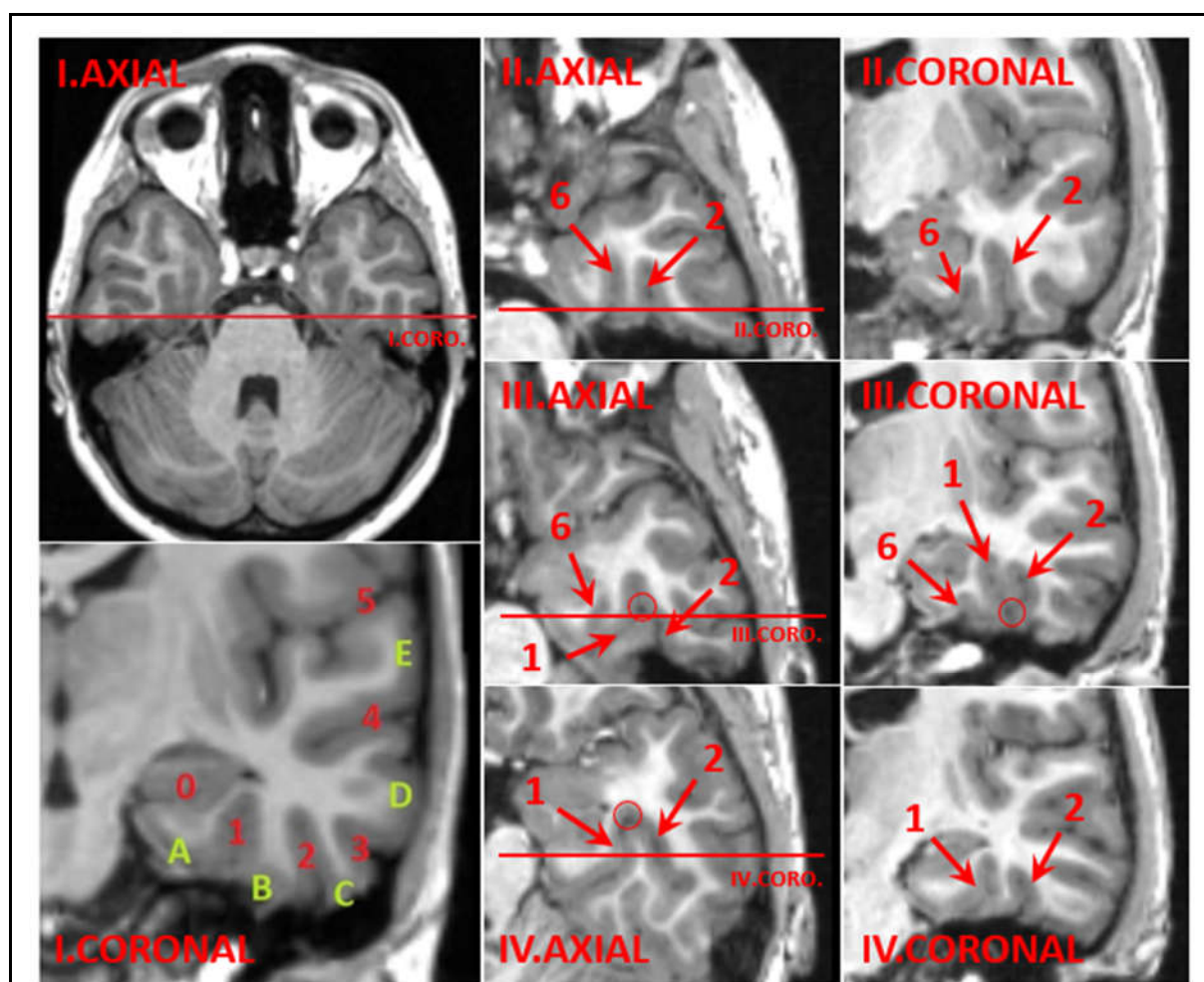


Figure 3. Temporal lobe anatomy and connection example

0 = Hippocampus; 1 = Collateral sulcus; 2 = Occipito-temporal sulcus; 3 = Inferior temporal sulcus; 4 = Superior temporal sulcus; 5 = Lateral sulcus; 6 = Rhinal sulcus;

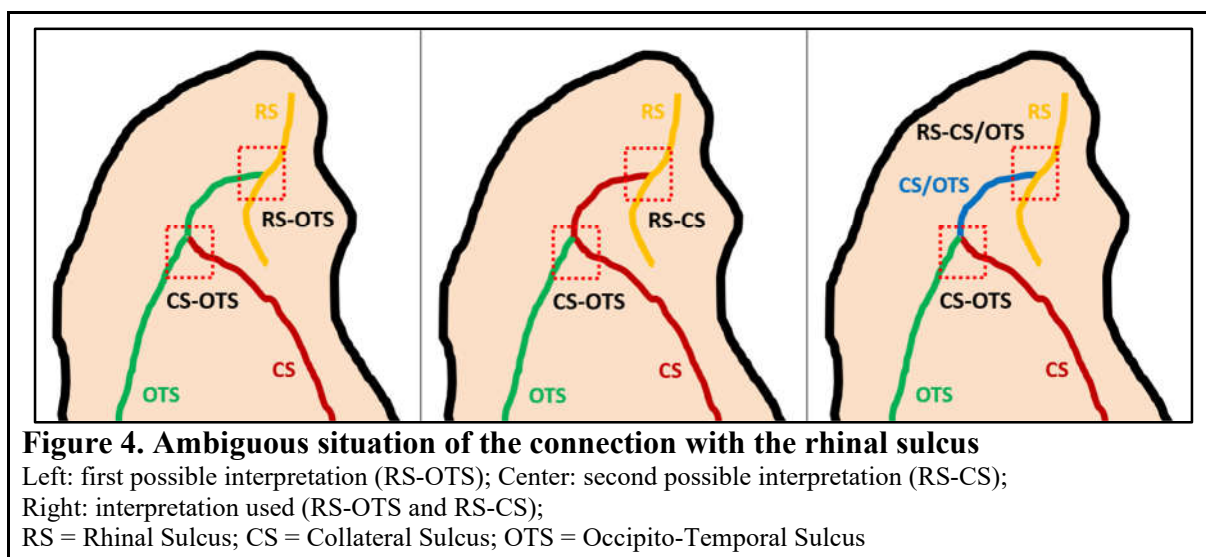
A = Hippocampal gyrus; B = Fusiform gyrus; C = Inferior temporal gyrus;

D = Middle temporal gyrus; E = Superior temporal gyrus

Images II to IV (axial and coronal views) are from the same subject. We can see a connection between the collateral sulcus and the occipito-temporal sulcus in III axial, III coronal and IV axial (red circle).

2.3.5. Ambiguous connection

A difficulty arises when the CS and OTS sulci merge and connect with RS, as it becomes difficult to know which of the CS or OTS connects with the RS (**Figure 4**). In this particular case, we rated that all sulci connect (RS-CS=1, CS-OTS=1 and RS-OTS=1).



2.4 Statistical analyses

2.4.1 Reproducibility of the classification (intra/inter-observer)

Kevin De Matos (KDM) performed manual assessment on all the MRI images. We estimated the intra-observer reproducibility on the first 100 IMAGEN individuals rated a second time by KDM. In addition, we estimated the inter-observer reproducibility thanks to a second rater (LC=Lydia Chougar, neuroradiologist) who evaluated the same 100 individuals. We reported the reproducibility using Cohen's kappa without weighting. For a better understanding, we have also reported the proportions of true positives / true negatives / false positives / false negatives compared with KDM.

2.4.2 Descriptive analysis of sulcal connections

First, we reported the frequency of each sulcal connection across the three databases. Next, we tested the association between sulcal polymorphisms and demographics or general variables

(sex, age, weight, height, intracranial volume (ICV), handedness, BMI and site). Then, we evaluated possible associations between sulcal polymorphisms and incomplete hippocampal inversions (IHI). For IMAGEN, the IHI data came from the manual rating used in the study by Cury et al. (2015) and for QTIM/QTAB the IHI data were manually rated by KDM using the protocol described in Cury et al.

We used a generalized linear model (GLM) for the statistical analysis and significance testing using the "statsmodels" python package. Specifically, we used a logistic regression as the sulcal connections were binary variables, and we reported the OR (odd-ratios), and p-value from the Wald/log-likelihood ratio test. We evaluated the correlations between sulcal connections and all general and demographic variables, using the joint model:

$$\text{Connections} \sim \text{age} + \text{sex} + \text{handedness} + \text{weight} + \text{height} + \text{location} + \text{ICV} + \text{BMI}$$

We used IMAGEN as a discovery sample and evaluated if the significant associations replicated in QTIM and QTAB. We used a significance threshold of $7.81 \times 10^{-4} = 0.05/64$ ($64 = (3 \text{ connections} + \text{nbr of connection}) \times 2 \text{ hemispheres} \times 8 \text{ demographic variables}$) tested in the discovery sample, which accounts for the number of tests performed (Bonferroni correction). As twins from the same family may not yield independent observations (a hypothesis of GLM modeling), we selected a single individual per family in the replication analyses. Similarly, when testing associations between sulcal polymorphisms and IHI, we used the model:

$$\text{IHI criteria} \sim \text{connections} + \text{age} + \text{sex} + \text{handedness} + \text{weight} + \text{height} + \text{location} + \text{ICV} + \text{BMI}$$

with $\text{connections} = \text{Left RS-CS} + \text{Left CS-OTS} + \text{Left RS-OTS} + \text{Right RS-CS} + \text{Right CS-OTS} + \text{Right RS-OTS}$, and we used a significance threshold of $3.57 \times 10^{-4} = 0.05/140$ ($140 = 5 \text{ IHI criteria} \times 2 \text{ hemispheres} \times 14 \text{ variables}$).

2.4.3 Heritability

We used the twin samples QTIM and QTAB to estimate the heritability of sulcal connections. The heritability quantifies how much of the individual differences (variance) in sulcal connections may be attributable to genetic differences. Heritability ranges between 0 and 1,

with 0 corresponding to a trait with no genetic influence, and 1 indicating that the genetic differences account for all of the trait variability in the population.

We first reported the intra-pair tetrachoric correlations estimated with the R programming packages "umx" (Bates, Maes, et Neale 2019) and "psych" (Revelle 2022). Tetrachoric correlation is best suited to quantify correlations between dichotomous variables of interest. Intra-pair correlations that are larger in MZ pairs than in DZ pairs suggest that a trait is heritable. Next, we estimated the heritability using ACE and ADE models (M. C. Neale et Cardon 2011; Verweij et al. 2012) with the R programming package "umx" and "openMx" (M. C. Neale et al. 2016). The ACE model decomposes the trait variance into additive genetic contributions (A), shared or familial environmental contributions (C) and a residual term (E), which includes individual specific environmental sources of variance as well as measurement error. The ADE model allows estimating the contribution of genetic dominant effects (D). In the case of an ADE model, the broad sense heritability corresponds to the A+D contributions, by opposition to the narrow sense heritability which consists of the sole additive genetic contribution. For both models, we used age, sex, weight, height and ICV as covariates.

2.4.4 Co-occurrence of sulcal connections

We also reported the co-occurrence between the different sulcal connections, either intra-hemispheric or inter-hemispheric. We estimated these co-occurrences, controlling for covariates, using a GLM with the following formula:

$$Connection1 \sim Connection2 + sex + handedness + weight + height + location + ICV + BMI$$

We used a significance threshold of $1.85e-04=0.05/270$ ($270 = 30$ possible co-occurrence combinations x 9 variables) tested in the discovery sample, which accounts for the number of tests performed (Bonferroni correction).

2.4.5 Genetic correlations

Lastly, we reported genetic correlations (r_G), estimated using twin models. Genetic correlations indicate how much of the genetic sources of variance may be common between the sulcal connections. In other words, how much are sulcal connections influenced by the same genetic variants. Note that we have calculated genetic correlations (between the traits liability, i.e. assuming a liability threshold model (B. Neale 2014)) in this section whereas the phenotypic co-occurrences are reported as odds ratio.

3. Results

3.1 Reproducibility of the radiological classification (intra/inter-observer)

All ratings, carried out in 100 IMAGEN individuals, showed a very good intra-rater reproducibility as indicated by $\kappa > 0.80$ (Table 2). The highest kappa was 0.93 (95%CI=0.88-0.98) for the CS-OTS connection. The RS-OTS connection exhibited the lowest kappa (0.83) although the confidence interval was wider (95%CI=0.70-0.96).

The different raters (KDM and LD) showed good agreement for the RS-CS (kappa=0.77) and CS-OTS (kappa=0.77) connections, and moderate agreement for the RS-OTS connection (kappa=0.48) (Table 2).

Table 2. Intra-observer and inter-observer reproducibility

	RS-CS	CS-OTS	RS-OTS
<u>Intra-observer</u>			
KDM1-KDM2: Kappa	0.87	0.93	0.83
CI (95%)	[0.80 - 0.94]	[0.88 - 0.98]	[0.70 - 0.96]
TP / TN / FP / FN	64 / 124 / 7 / 5	88 / 105 / 3 / 4	17 / 177 / 1 / 5
<u>Inter-observer</u>			
KDM1-LC: Kappa	0.77	0.77	0.48
CI (95%)	[0.68 - 0.86]	[0.68 - 0.86]	[0.31 - 0.65]
TP / TN / FP / FN	61 / 118 / 13 / 8	88 / 89 / 19 / 4	16 / 158 / 20 / 6
KDM2-LC: Kappa	0.79	0.76	0.45
CI (95%)	[0.71 - 0.88]	[0.67 - 0.85]	[0.28 - 0.62]
TP / TN / FP / FN	63 / 118 / 11 / 8	87 / 89 / 20 / 4	14 / 160 / 22 / 4

RS = Rhinal Sulcus; CS = Collateral Sulcus; OTS = Occipito-Temporal Sulcus;
 KDM1 = First evaluation of observer KDM; KDM2 = Second evaluation; LC = Evaluation of observer LC;
 TP/TN/FP/FN = True Positive/True Negative/False Positive/False Negative with first observer considered as
 reference; CI = Confidence Interval (95%)

3.2 Descriptive analysis of sulcal connections

3.2.1 Descriptive analysis: Frequency

We observed that the frequencies of the sulcal connections were comparable across the three different samples (based on overlapping confidence intervals in most cases, **Figure 5**). In the left hemisphere, the CS-OTS connection was the most frequent (55-60%), followed by the RS-CS connection (35-40%) and the RS-OTS connection (5-10%). In the right hemisphere, the RS-CS connection was the most frequent (30-35%), followed by the CS-OTS connection (25-30%) and the RS-OTS connection (5-10%) (**Figure 5, Table 3**).

In the left hemisphere, for IMAGEN, 18.2% of individuals had zero connections, 57.3% had a single connection, 20.3% had two while 4.2% had three connections (which includes the ambiguous case). For QTIM+QTAB, these figures were respectively 23.4%, 54.3%, 21.0%, and 1.4%. In the right hemisphere, for IMAGEN, 36.2% of individuals had zero connections, 52.4% had a single connection, 9.0% had two while 2.3% had three connections. For QTIM+QTAB, these figures were respectively 42.3%, 47.5%, 10.0%, and 0.2%. See **Table S2** for separate frequencies of QTIM and QTAB, and see **Table S3** and **Figure S3** for frequencies by pattern in supplementary materials.

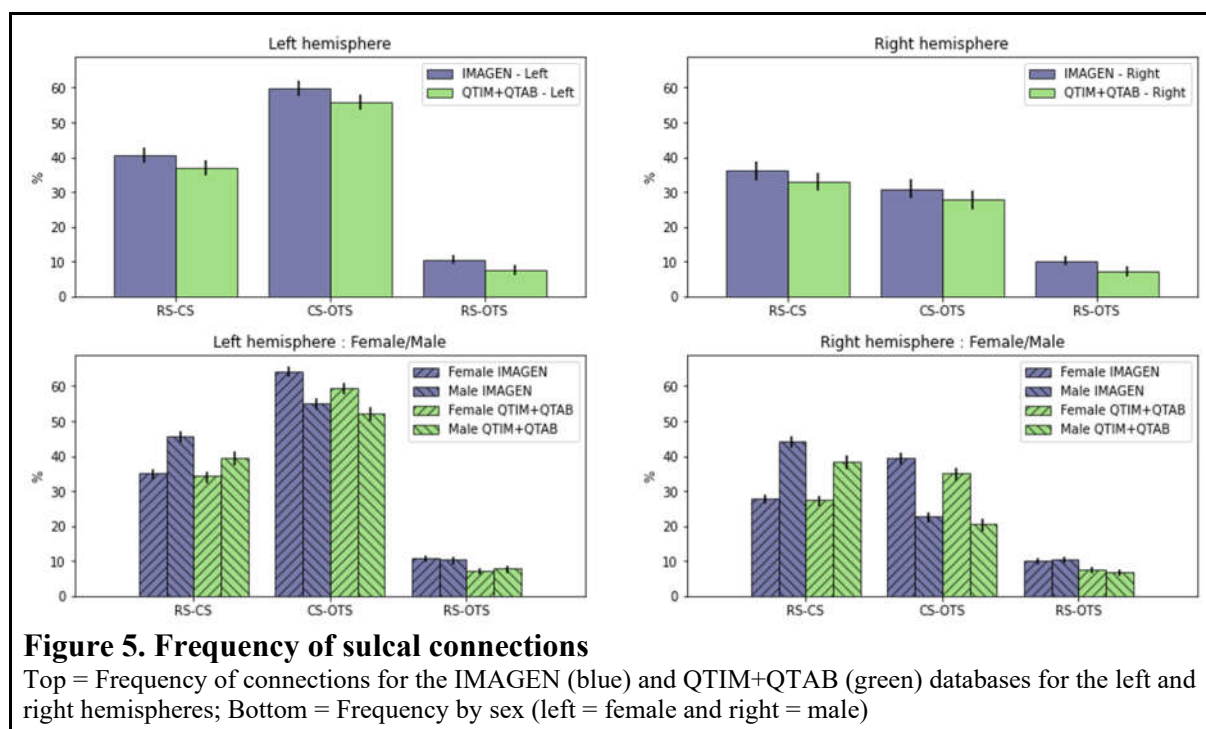


Table 3. Frequency of connections with total number

	Left hemisphere		Right hemisphere	
	IMAGEN	QTIM+QTAB	IMAGEN	QTIM+QTAB
RS-CS % (N)	40.3 (807)	36.4 (504)	35.8 (718)	32.0 (443)
Total / F / M	35.0 (360)	34.2 (275)	27.9 (287)	27.4 (220)
	45.8 (447)	39.5 (229)	44.2 (431)	38.5 (223)
CS-OTS % (N)	59.8 (1,198)	56.4 (781)	31.1 (624)	28.9 (400)
Total / F / M	64.3 (661)	59.6 (478)	39.3 (404)	35.0 (281)
	55.0 (537)	52.2 (303)	22.5 (220)	20.5 (119)
RS-OTS % (N)	10.6 (212)	7.4 (103)	10.2 (205)	7.3 (101)
Total / F / M	10.8 (111)	7.1 (57)	9.9 (102)	7.6 (61)
	10.3 (101)	7.9 (46)	10.5 (103)	6.9 (40)
Number of connections = 0	18.2 (364)	23.4 (324)	36.2 (726)	42.3 (585)
Total / F / M	18.4 (189)	22.5 (181)	36.6 (376)	41.4 (333)
% (N) Total / F / M	17.9 (175)	24.7 (143)	35.9 (350)	43.4 (252)
Number of connections = 1	57.3 (1,148)	54.3 (751)	52.4 (1,051)	47.5 (657)
Total / F / M	57.3 (589)	55.1 (443)	51.9 (534)	47.6 (383)
% (N) Total / F / M	57.3 (559)	53.1 (308)	53.0 (517)	47.2 (274)
Number of connections = 2	20.3 (407)	21.0 (290)	9.0 (180)	10.0 (139)
Total / F / M	20.1 (207)	21.5 (173)	8.9 (92)	10.6 (85)
% (N) Total / F / M	20.5 (200)	20.2 (117)	9.0 (88)	9.3 (54)
Number of connections = 3	4.2 (85)	1.4 (19)	2.3 (47)	0.2 (3)
Total / F / M	4.2 (43)	0.9 (7)	2.5 (26)	0.4 (3)
% (N) Total / F / M	4.3 (42)	2.1 (12)	2.2 (21)	0.0 (0)

First line (bold) = Total frequency; Second line = Female frequency; Third line = Male frequency;
 RS = Rhinal Sulcus; CS = Collateral Sulcus; OTS = Occipito-Temporal Sulcus; F = Female; M = Male

3.2.2 Descriptive analysis: Demographic GLM model with replication

In the GLM model, after Bonferroni correction (significance threshold of $7.81e-04$), we found in IMAGEN that the sulcal connection frequency was strongly associated with sex, in particular for the right RS-CS connection (28% in females, 44% in males, OR=2.0 p-value= $1.41e-08$, controlling for all other covariates) and CS-OTS connection (39% in females, 23% in males, OR = 0.5 and p-value = $1.15e-07$). In the left hemisphere, the RS-CS connection was also more common in males (35% in females, 46% in males, OR=1.55 and p-value= $2.19e-04$) (Table 3-4 and Figure 5).

We replicated the sexual dimorphism of the right CS-OTS in QTIM+QTAB (35% in females, 21% in males, OR=0.51 and p-value= $5.06e-03$); the other associations failed to replicate (right RS-CS: 27% in females, 39% in males, OR=1.13, p-value=0.57; left RS-CS: 34% in females, 40% in males, OR=0.73, p-value=0.13).

Table 4. IMAGEN: GLM of demographic data

	age (year)	sex (female vs. male)	handedness	weight (kg)	height (kg)	site*	ICV (mm ³)	BMI (kg/m ²)
Right hemisphere								
RS-CS:	0.86	2.0		1.04	0.98		1.0	0.92
OR (p-value)	(0.21)	(1.41e-08)	(0.85)	(0.5)	(0.56)	(0.92)	(0.93)	(0.58)
CS-OTS:	1.14	0.5		1.02	0.97		1.0	0.92
OR (p-value)	(0.28)	(1.15e-07)	(0.2)	(0.76)	(0.41)	(0.07)	(0.83)	(0.6)
RS-OTS:	1.27	1.19		1.11	0.9		1.0	0.76
OR (p-value)	(0.18)	(0.36)	(0.31)	(0.16)	(0.06)	(0.96)	(0.56)	(0.19)
Nbr connections:	1.02	1.03		1.03	0.98		1.0	0.93
OR (p-value)	(0.67)	(0.42)	(0.17)	(0.15)	(0.06)	(0.33)	(0.87)	(0.14)
Left hemisphere								
RS-CS:	0.86	1.55		1.07	0.95		1.0	0.84
OR (p-value)	(0.19)	(2.19e-04)	(0.94)	(0.17)	(0.17)	(0.19)	(0.76)	(0.23)
CS-OTS:	0.92	0.75		0.94	1.03		1.0	1.16
OR (p-value)	(0.43)	(1.49e-02)	(0.9)	(0.23)	(0.4)	(0.41)	(0.76)	(0.29)
RS-OTS:	0.89	1.05		1.05	0.96		1.0	0.85
OR (p-value)	(0.51)	(0.8)	(0.96)	(0.5)	(0.44)	(0.56)	(0.86)	(0.46)
Nbr connections:	0.93	1.04		1.01	0.99		1.0	0.98
OR (p-value)	(0.1)	(0.35)	(0.94)	(0.7)	(0.5)	(0.23)	(0.94)	(0.7)

First line = Odds ratio; Second line = uncorrected p-value (significance threshold of $7.81e-04$); in bold if significant; RS = Rhinal Sulcus; CS = Collateral Sulcus; OTS = Occipito-Temporal Sulcus
F = Female; M = Male; OR = odds ratio. We do not provide odds ratios for sites as there are 8 different sites.
The p-value corresponds to a single omnibus test for all the sites.

3.2.3 Descriptive analysis: IHI GLM model with replication

In the analysis of association between sulcal connections and IHI, after Bonferroni correction (significance threshold of $3.57e-04$), on the ipsilateral side, a more vertical and deep collateral sulcus (C2 criterion) was significantly associated with the presence of RS-CS (left: OR=1.34 and p-value= $3.26e-34$, right: OR=1.16 and p-value= $5.13e-15$) and CS-OTS (left: OR=1.22 and p-value= $6.72e-20$, right: OR=1.11 and p-value= $1.99e-08$) connections on both hemispheres. A more medial positioning of the hippocampal body (C3 criterion) was significantly associated with the presence of RS-CS (left: OR=1.16 and p-value= $1.98e-07$, right: OR=1.14 and p-value= $8.50e-07$) and CS-OTS (left: OR=1.22 and p-value= $1.91e-15$, right: OR=1.17 and p-value= $1.33e-10$) connections. A fusiform gyrus with less deep sulci (C5 criterion) was significantly associated with the left RS-CS connection (OR=0.75 and p-value= $8.22e-10$) (Table 5). The contralateral side showed partly the same association but with lower odds ratios. In Table 6, we found that replication with QTIM and QTAB was satisfactory for the left hemisphere with odds ratios going in the same direction and also statistically significant. The right hemisphere gives less consistent replication results with four of the seven odds ratios close to one and becoming non-significant.

Table 5. IMAGEN: GLM of connections vs IHI

	RS-CS (L)	CS-OTS (L)	RS-OTS (L)	RS-CS (R)	CS-OTS (R)	RS-OTS (R)
Left hemisphere IHI						
C1:	0.93	0.98	1.08	0.97	1.08	0.92
OR (p-value)	(7.36e-03)	(0.35)	(4.33e-02)	(0.30)	(4.55e-03)	(3.68e-02)
C2:	1.34	1.22	1.01	1.11	1.2	0.91
OR (p-value)	(3.26e-34)	(6.72e-20)	(0.83)	(1.18e-05)	(8.93e-16)	(5.68e-03)
C3:	1.16	1.22	1.0	1.05	1.16	0.94
OR (p-value)	(1.98e-07)	(1.91e-15)	(0.91)	(0.09)	(6.72e-08)	(0.13)
C5:	0.75	0.9	1.12	0.95	0.99	0.96
OR (p-value)	(8.22e-10)	(1.34e-02)	(0.07)	(0.33)	(0.80)	(0.48)
SCi:	1.13	1.31	1.18	1.09	1.53	0.77
OR (p-value)	(0.21)	(1.88e-03)	(0.21)	(0.40)	(5.60e-06)	(0.05)
Right hemisphere IHI						
C1:	0.97	0.98	1.03	0.97	0.99	1.0
OR (p-value)	(0.15)	(0.25)	(0.37)	(0.15)	(0.46)	(0.92)
C2:	1.11	1.09	0.99	1.16	1.11	0.95
OR (p-value)	(7.11e-09)	(3.85e-07)	(0.66)	(5.13e-15)	(1.99e-08)	(3.57e-02)
C3:	1.07	1.11	1.01	1.14	1.17	0.91
OR (p-value)	(1.33e-02)	(6.55e-06)	(0.76)	(8.50e-07)	(1.33e-10)	(6.93e-03)
C5:	0.89	0.98	1.06	0.93	0.90	0.89
OR (p-value)	(6.59e-04)	(0.44)	(0.21)	(4.77e-02)	(7.84e-04)	(1.58e-02)
SCi:	1.0	1.17	1.06	1.23	1.12	0.79
OR (p-value)	(0.96)	(1.49e-02)	(0.55)	(5.84e-03)	(0.10)	(1.73e-02)

First line = Odds ratio; Second line = uncorrected p-value (significance threshold of 3.57e-04); in bold if significant; RS = Rhinal Sulcus; CS = Collateral Sulcus; OTS = Occipito-Temporal Sulcus; OR = odds ratio; IHI = incomplete hippocampal inversions; C1 = Verticality and roundness of the hippocampal body; C2 = Verticality and depth of the collateral sulcus; C3 = Medial positioning of the hippocampal body; C5 = depth of the sulci of the Fusiform Gyrus (collateral and occipito-temporal sulci); SCi = Sum of grades of individual criteria (C1-C5)

Table 6. GLM of connections vs IHI - Replication (QTIM+QTAB)

	RS-CS (L)	CS-OTS (L)	RS-OTS (L)	RS-CS (R)	CS-OTS (R)	RS-OTS (R)
Left hemisphere IHI						
C1:						
OR (p-value)	-	-	-	-	-	-
C2:	1.53	1.11	-	1.10	1.07	-
OR (p-value)	(1.32e-47)	(1.20e-04)	-	(2.04e-03)	(2.00e-02)	-
C3:	1.18	1.14	-	-	1.09	-
OR (p-value)	(1.13e-09)	(1.04e-07)	-	-	(2.09e-03)	-
C5:	0.72	-	-	-	-	-
OR (p-value)	(2.65e-09)	-	-	-	-	-
SCi:					1.25	-
OR (p-value)	-	-	-	-	(1.94e-02)	-
Right hemisphere IHI						
C1:						
OR (p-value)	-	-	-	-	-	-
C2:	1.12	1.01	-	1.31	1.0	-
OR (p-value)	(8.20e-06)	(0.57)	-	(9.52e-24)	(1.0)	-
C3:	-	1.05	-	1.05	1.14	-
OR (p-value)	-	(0.06)	-	(0.11)	(2.98e-06)	-
C5:	-	-	-	-	-	-
OR (p-value)	-	-	-	-	-	-
SCi:						
OR (p-value)	-	-	-	-	-	-

Only significant values of table 5 have been tested; First line = Odds ratio; Second line = p-value; in bold if significant; RS = Rhinal Sulcus; CS = Collateral Sulcus; OTS = Occipito-Temporal Sulcus; OR = odds ratio; IHI = incomplete hippocampal inversions; C1 = Verticality and roundness of the hippocampal body; C2 = Verticality and depth of the collateral sulcus; C3 = Medial positioning of the hippocampal body; C5 = depth of the sulci of the Fusiform Gyrus (collateral and occipito-temporal sulci); SCi = Sum of grades of individual criteria (C1-C5)

3.3 Heritability

Table 7. Tetrachoric correlation

	MZ	DZ	MZMM	MZFF	DZMM	DZFF	DZMF/FM
Left hemisphere							
RS-CS	0.69	0.01	0.83	0.55	-0.24	0.31	-0.16
CI (95%)	[0.51 - 0.78]	[-0.19 - 0.17]	[0.67 - 0.95]	[0.30 - 0.72]	[-0.58 - 0.11]	[0.05 - 0.66]	[-0.50 - 0.10]
CS-OTS	0.48	0.27	0.34	0.59	-0.09	0.22	0.48
CI (95%)	[0.30 - 0.63]	[0.12 - 0.39]	[0.07 - 0.65]	[0.39 - 0.75]	[-0.40 - 0.42]	[-0.12 - 0.56]	[0.18 - 0.73]
RS-OTS	-0.04	0.02	-	-	-	-	-
CI (95%)	[-0.31 - 0.28]	[-0.31 - 0.36]	-	-	-	-	-
<p>Detailed description of the forest plot for the left hemisphere: The plot shows tetrachoric correlations for three sulcus pairs: RS-CS, CS-OTS, and RS-OTS. For each pair, data is shown for MZ (Monozygotic) and DZ (Dizygotic) twins, and for DZMF/FM (Dizygotic Male and Female) twins. The plot is further stratified by 'All' (yellow), 'Male' (purple), and 'Female' (green) subjects. Error bars represent 95% confidence intervals. The y-axis ranges from -0.6 to 1.0.</p>							
	MZ	DZ	MZMM	MZFF	DZMM	DZFF	DZMF/FM
Right hemisphere							
RS-CS	0.53	-0.07	0.47	0.56	0.10	0.20	-0.45
CI (95%)	[0.33 - 0.69]	[-0.32 - 0.17]	[0.22 - 0.73]	[0.34 - 0.83]	[-0.34 - 0.57]	[-0.13 - 0.46]	[-0.73 - -0.19]
CS-OTS	0.53	0.26	0.42	0.55	0.03	0.26	0.28
CI (95%)	[0.34 - 0.68]	[0.03 - 0.47]	[0.06 - 0.73]	[0.30 - 0.77]	[-0.42 - 0.44]	[-0.10 - 0.57]	[-0.04 - 0.59]
RS-OTS	0.14	0.17	-	-	-	-	-
CI (95%)	[-0.24 - 0.49]	[-0.21 - 0.48]	-	-	-	-	-
<p>Detailed description of the forest plot for the right hemisphere: The plot shows tetrachoric correlations for three sulcus pairs: RS-CS, CS-OTS, and RS-OTS. For each pair, data is shown for MZ (Monozygotic) and DZ (Dizygotic) twins, and for DZMF/FM (Dizygotic Male and Female) twins. The plot is further stratified by 'All' (yellow), 'Male' (purple), and 'Female' (green) subjects. Error bars represent 95% confidence intervals. The y-axis ranges from -0.8 to 0.8.</p>							

RS = Rhinal Sulcus; CS = Collateral Sulcus; OTS = Occipito-Temporal Sulcus; OR = odds ratio;

MZ = Monozygotic; DZ = Dizygotic; MZMM / MZFF = Monozygotic Male / Female;

DZMM / DZFF = Dizygotic Male / Female; DZMF/FM = Dizygotic Male and Female.

The **Table 7** presents the tetrachoric correlations in the pairs of monozygotic (MZ) and dizygotic (DZ) twins resulting from the addition of the QTIM and QTAB databases with their confidence intervals as well as the separation of the male/female data.

3.3.1 Twin pair tetrachoric correlation

In **Table 7**, showing the within-pair tetrachoric correlations, we observed a seemingly larger correlation between monozygotic (MZ) twins than between dizygotic (DZ) twins for the RS-CS and CS-OTS connections on both sides. Note that $MZ > 2 * DZ$ (e.g. for left RS-CS) suggests a non-additive (e.g. dominant) genetic contribution. The negative tetrachoric correlation for opposite sex pairs, might suggest a sex-limitation model, even if the confidence intervals remained wide, considering the current sample size. On the other hand, we found no evidence of twin pair correlation for the RS-OTS suggesting little heritability or at an undetectable level considering the current sample size.

3.3.2 Heritability: ACE and ADE models

We fitted both ACE and ADE models and used the model with the lowest AIC value (“best fitting”) to further test the significance of A and C/D (**Table 8**). The ADE model was the best fitting for left and right RS-CS and the DE sub-model gave the lowest AIC value (left RS-CS: $D=0.45$ 95%CI=0.36–0.54, right RS-CS: $D=0.30$ 95%CI=0.25–0.41). The ACE model was the best fitting for left CS-OTS and the AE model gave the lowest AIC value ($A=0.30$ 95%CI=0.20–0.40) while the ADE model was the best fitting for right CS-OTS and the AE model gave the lowest AIC value ($A=0.28$ 95%CI=0.17–0.38). In line with the tetrachoric correlation, the RS-OTS connections on both sides showed little to no heritability.

Table 8. ACE and ADE models

		Parameter estimates			Model fit				
Variable	Model	A	C/D	E	PE	delta-df	-2LL	p-value	AIC
RS-CS (L)	ACE	0.40 [0.28 - 0.49]	0 [0 - 0.07]	0.60 [0.51 - 0.71]	10	-	1301.08	-	1321.08
	ADE	0 [0 - 0.23]	0.45 [0.36 - 0.54]	0.55 [0.46 - 0.65]	10	-	1292.57	-	1312.57
	AE	0.40 [0.29 - 0.49]	-	0.60 [0.51 - 0.71]	9	1	1301.08	0.004	1319.08
	DE	-	0.45 [0.36 - 0.54]	0.55 [0.46 - 0.65]	9	1	1292.57	1.000	1310.57
CS-OTS (L)	ACE	0.28 [0 - 0.40]	0.02 [0 - 0.27]	0.70 [0.60 - 0.82]	10	-	1396.40	-	1416.40
	ADE	0.30 [0.20 - 0.40]	0 [0 - 0.39]	0.70 [0.60 - 0.80]	10	-	1396.43	-	1416.43
	AE	0.30 [0.20 - 0.40]	-	0.70 [0.60 - 0.80]	9	1	1396.43	0.885	1414.43
	CE	-	0.22 [0.15 - 0.31]	0.78 [0.69 - 0.86]	9	1	1399.30	0.089	1417.30
RS-OTS (L)	ACE	0 [0 - 0.11]	0 [0 - 0.08]	1 [1 - 1]	10	-	204.99	-	224.99
	ADE	0 [0 - 0.11]	0 [0 - 0.12]	1 [1 - 1]	10	-	204.99	-	224.99
RS-CS (R)	ACE	0.26 [0.15 - 0.36]	0 [0 - 0.09]	0.74 [0.64 - 0.85]	10	-	1252.51	-	1272.51
	ADE	0 [0 - 0.25]	0.30 [0.05 - 0.41]	0.70 [0.59 - 0.80]	10	-	1248.09	-	1268.09
	AE	0.26 [0.16 - 0.36]	-	0.74 [0.64 - 0.85]	9	1	1252.51	0.035	1270.51
	DE	-	0.30 [0.25 - 0.41]	0.70 [0.59 - 0.80]	9	1	1248.09	1.000	1266.09
CS-OTS (R)	ACE	0.28 [0 - 0.38]	0 [0 - 0.23]	0.72 [0.62 - 0.83]	10	-	1199.43	-	1219.43
	ADE	0.24 [0 - 0.38]	0.05 [0 - 0.39]	0.72 [0.61 - 0.80]	10	-	1199.39	-	1219.39
	AE	0.28 [0.17 - 0.38]	-	0.72 [0.62 - 0.83]	9	1	1199.43	0.855	1217.43
	DE	-	0.30 [0.25 - 0.40]	0.70 [0.60 - 0.81]	9	1	1200.29	0.343	1218.29
RS-OTS (R)	ACE	0 [0 - 0.16]	0.05 [0 - 0.13]	0.95 [0.87 - 1]	10	-	206.26	-	226.26
	ADE	0.05 [0 - 0.17]	0 [0 - 0.17]	0.95 [0.83 - 1]	10	-	206.50	-	226.50

In bold = best fitting between ACE and ADE models; in bold and underlined = best fitting of all;

RS = Rhinal Sulcus; CS = Collateral Sulcus; OTS = Occipito-Temporal Sulcus;

A = Additive genetic effects; D = Dominance genetic effects; C = Shared environmental effects;

E = Non-shared environmental effects; PE = number of estimate parameters in model; df = Degrees of freedom;

-2LL = twice the negative log-likelihood; AIC = Akaike's Information Criterion

3.4. Co-occurrence of sulcal connections

Table 9 presents the co-occurrence of sulcal connections. Overall, after Bonferroni correction (significance threshold of $1.85e-04$), we found the strongest correlations between the same type of connection in the left and right hemispheres (e.g. left RS-CS: OR=12.12 and p-value= $2.38e-96$ with the right RS-CS). The third line represents the co-occurrence in percentage (e.g. when left RS-CS was present, left CS-OTS was also present at 49.2% but when left CS-OTS was present, left RS-CS was also present at only 33%). In **Table 10**, the replication with QTIM+QTAB confirmed to us that the same type of connection in the left and right hemispheres remained significant (e.g. left RS-CS: OR=16.22 and p-value= $6.74e-43$ with the right RS-CS).

Table 9. IMAGEN: GLM of connections

	RS-CS (L)	CS-OTS (L)	RS-OTS (L)	RS-CS (R)	CS-OTS (R)	RS-OTS (R)
RS-CS (L):		0.50	2.56	12.12 (2.38e-	0.94	1.53
OR (p-value)	-	(2.56e-12)	(2.22e-09)	96)	(0.57)	(6.61e-03)
%		49.2	16.2	67.2	28.8	12.7
CS-OTS (L):	0.50		1.39	0.53	6.15	1.02
OR (p-value)	(2.55e-12)	-	(4.39e-02)	(4.39e-10)	(4.30e-41)	(0.89)
%	33.0		12.0	29.3	44.0	10.3
RS-OTS (L):	2.57	1.38		1.91	1.34	6.89
OR (p-value)	(2.16e-09)	(4.45e-02)	-	(3.51e-05)	(0.07)	(2.39e-26)
%	60.3	66.5		49.0	36.6	34.5
RS-CS (R):	12.17 (2.61e-	0.53	1.91		0.46	1.91
OR (p-value)	96)	(4.47e-10)	(3.63e-05)	-	(1.15e-10)	(5.27e-05)
%	75.4	49.1	14.8		19.6	14.2
CS-OTS (R):	0.94	6.15	1.34	0.46		1.26
OR (p-value)	(0.56)	(4.96e-41)	(0.07)	(1.09e-10)	-	(0.17)
%	37.4	85.3	12.8	22.7		11.9
RS-OTS (R):	1.53	1.02	6.87	1.90	1.26	
OR (p-value)	(6.88e-03)	(0.89)	(2.64e-26)	(5.63e-05)	(0.17)	-
%	49.7	60.0	36.2	49.2	35.7	

First line = Odds ratio; Second line = uncorrected p-value (significance threshold = 1.85e-04);
Third line = co-occurrence in percentage; in bold if significant; RS = Rhinal Sulcus; CS = Collateral Sulcus;
OTS = Occipito-Temporal Sulcus; OR = odds ratio; L = Left; R = Right

Table 10. Replication in QTIM+QTAB

	RS-CS (L)	CS-OTS (L)	RS-OTS (L)	RS-CS (R)	CS-OTS (R)	RS-OTS (R)
RS-CS (L):		0.65	0.67	16.22 (6.74e-		
OR (p-value)	-	(5.75e-03)	(0.22)	43)	-	-
%		48.1	6.3	65.7		
CS-OTS (L):	0.65			0.57	13.3	
OR (p-value)	(5.75e-03)	-	-	(6.76e-04)	(1.07e-23)	-
%	30.7			25.8	45.8	
RS-OTS (L):	0.66			1.42		7.26
OR (p-value)	(0.2)	-	-	(0.26)	-	(3.31e-08)
%	29.5			31.6		24.2
RS-CS (R):	16.12 (5.52e-	0.57	1.43		0.6	0.99
OR (p-value)	43)	(7.09e-04)	(0.24)	-	(9.63e-03)	(0.96)
%	74.4	45.8	7.7		20.2	6.4
CS-OTS (R):		13.3		0.59		
OR (p-value)	-	(9.99e-24)	-	(7.67e-03)	-	-
%		89.1		22.1		
RS-OTS (R):			7.3	0.97		
OR (p-value)	-	-	(3.00e-08)	(0.92)	-	-
%			25.3	27.5		

Only significant values of table 8 have been tested; First line = Odds ratio; Second line = p-value;
Third line = co-occurrence in percentage; in bold if significant; RS = Rhinal Sulcus; CS = Collateral Sulcus;
OTS = Occipito-Temporal Sulcus; OR = odds ratio; L = Left; R = Right

3.5 Genetic correlations

We estimated the genetic correlation (A) for each pair of two connections. In detail, we detected a high and significant correlations between left/right CS-OTS connections ($A=1.00$, $95\%CI=0.80-1.00$ and $p\text{-value}=7.00e-12$) and between left/right RS-CS connections ($A=0.94$, $95\%CI=0.78-1.00$ and $p\text{-value}=4.80e-11$) (**Table 11**). It was the same connection pairs that obtained the highest odds ratios for the co-occurrence. The RS-OTS connections on both sides have not been tested due to lack of heritability. We also estimated the environmental correlation (E) giving several significant results but weak correlations.

Table 11. Genetic correlations

	RS-CS (L)	CS-OTS (L)	RS-OTS (L)	RS-CS (R)	CS-OTS (R)	RS-OTS (R)
RS-CS (L):		A = -0.26		A = 0.94	A = -0.23	
CI (95%)	-	[-0.51 - -0.03]	NA	[0.78 - 1.00]	[-0.50 - 0.02]	NA
(p-value)		(2.90e-02)		(4.80e-11)	(6.64e-02)	
CS-OTS (L):	E = -0.01			A = -0.31	A = 1.00	
CI (95%)	[-0.12 - 0.10]	-	NA	[-0.60 - -0.02]	[0.80 - 1.00]	NA
(p-value)	(8.56e-01)			(3.53e-02)	(7.00e-12)	
RS-OTS (L):						
CI (95%)	NA	NA	-	NA	NA	NA
(p-value)						
RS-CS (R):	E = 0.36	E = -0.03			A = -0.44	
CI (95%)	[0.29 - 0.45]	[-0.14 - 0.08]	NA	-	[-0.79 - -0.14]	NA
(p-value)	(5.27e-14)	(6.31e-01)			(4.54e-03)	
CS-OTS (R):	E = 0.11	E = 0.17		E = 0.03		
CI (95%)	[0.00 - 0.22]	[0.09 - 0.25]	NA	[-0.08 , 0.13]	-	NA
(p-value)	(4.61e-02)	(1.15e-04)		(6.32e-01)		
RS-OTS (R):						
CI (95%)	NA	NA	NA	NA	NA	-
(p-value)						

First line = Genetic correlation (A) or Environmental correlation (E); Second line = Confidence Interval (95%); Third line = p-value; in bold if significant; NA (Not Applicable) = Confidence interval between -1 and 1; RS = Rhinal Sulcus; CS = Collateral Sulcus; OTS = Occipito-Temporal Sulcus; L = Left; R = Right

4. Discussion

In this study, we introduced a simple manual classification of the morphological variations of the rhinal, collateral and occipito-temporal sulci by focusing only on their mutual connections. We have obtained many novel results: precise characterization of sulcal connection frequencies with evidence of important hemispheric and sexual differences as well as evidence of moderate broad-sense heritability for two of the connections with also the sharing of genetic and environmental causal factors. Our classification is modular and may be extended to other sulci and lobes.

We showed using multiple raters that our classification was reproducible, in particular for the RS-CS ($\kappa=0.77$) and CS-OTS ($\kappa=0.77$) connections (**Table 2**). Reproducibility was lower for the RS-OTS connection ($\kappa=0.48$), possibly due to ambiguous situations and a rarer phenotype.

We performed a radiological evaluation of nearly 3,400 healthy young individuals from three databases. We reported precise frequency of each connection between sulci (**Table 3**). Thanks to our approach, we have for the first time quantified this on a large-scale. This is in itself a novel contribution to neuroanatomical knowledge, and it could serve as a basis for future research (for example by comparing our results with databases of patients with various neurological diseases, by using our data to create automated classification methods, by increasing the number of sulcus taken into account, etc.). Moreover, the hemispheric differences found would be in support of different sulcal development patterns between hemispheres. Indeed, there was, for the left hemisphere, a frequency of 55-60% for the CS-OTS connection and 35-40% for the RS-CS connection while, for the right hemisphere, there was a frequency of 30-35% for RS-CS connection and 25-30% for CS-OTS connection. We therefore found that sulcal connections were more frequent in the left hemisphere. On this subject, the ENIGMA-Laterality Working Group has published several studies of brain asymmetries (Guadalupe et al. 2017; X. Kong et al. 2022). In particular, the study by X.-Z. Kong et al. (2018) focused on

cortical thickness and surface area in 17,141 healthy subjects. It revealed global hemispheric asymmetries, with thicker cortex in the left hemisphere but smaller cortical surface area. At the regional level, many asymmetries were reported, including some in the anterior temporal lobe. The entorhinal cortex and the temporal pole tended to be thicker in the right hemisphere, but the cortical surface area of all gyri (inferior temporal, fusiform, entorhinal, and parahippocampal) appeared larger in the left hemisphere. More work is needed to evaluate whether these asymmetries could be associated with the asymmetries in sulcal connections we reported here.

Unexpectedly, when individuals were grouped by sex, we found large frequency differences for CS-OTS and RS-CS connections (**Table 3 and 4**). Specifically, the left and right RS-CS connections were significantly more frequent in males (left RS-CS: 35% in females, 46% in males, OR=1.55 and p-value=2.19e-04; right RS-CS: 28% in females, 44% in males, OR=2.0 and p-value=1.41e-08) and the right CS-OTS connection was more common in females (39% in females, 23% in males, OR = 0.5 and p-value = 1.15e-07). At this level, it is difficult to understand the underlying mechanisms responsible for these differences. However, we ruled out that this sexual dimorphism could be explained by intracranial volume or other demographic data. However, we only replicated the sexual dimorphism (using QTIM+QTAB) of the right CS-OTS (35% in females, 21% in males, OR=0.51 and p-value= 5.06e-03). To our knowledge, our study is the largest to date to study sulci connection and the first one to report precise frequency in the general population as well as a sex difference. The study of Novak et al. (2002), with a partially compatible classification, used 50 individuals MRIs, and highlighted a sexual dimorphism for the RS-CS connection which went in the same direction as our study (more frequent in men than in women) and concluded that the sex of individuals was a significant factor in sulcal patterns. Other studies done in the meantime have not confirmed this tendency. This sexual dimorphism may also relate to previous reports of sexual dimorphism in the brain. It is well established that males have on average a 10-12% larger total brain volume (Ruigrok

et al. 2014; Kruggel et Solodkin 2020) as well as larger cortical surface area, while females tend to exhibit thicker cortical thickness (Ritchie et al. 2018). At a regional level, those sexual differences are observed throughout the anterior temporal pole, but are greatly reduced when controlling for intracranial volume differences (Ritchie et al. 2018). In addition, sex was also associated with brain asymmetry, with males showing more asymmetry in cortical thickness of the parahippocampal and entorhinal gyri, as well as less asymmetry in surface area (X.-Z. Kong et al. 2018). Finally, several psychiatric and behavioral dimensions are associated with sex, and more studies are required to understand their relationships with brain sexual dimorphism.

In addition, we did not observe an association between sulcal connection and handedness, although the association may be small and undetectable with current statistical power. The ENIGMA consortium came to a similar conclusion when looking at cortical thickness, cortical surface area (X.-Z. Kong et al. 2018) or the volume of subcortical structures (Guadalupe et al. 2017).

Our work follows and extends that of four other published studies, that studied sulci connection and used a compatible classification system (Kim et al. 2008; Huntgeburth et Petrides 2012; Cikla et al. 2016; Ovalioglu et al. 2018) (**Table S4**). The number of participants in those studies were small, varying between 18 and 51, leading to wide confidence intervals of frequency estimate (**Table S4**). Overall, the studies of Cikla et al. and Ovalioglu et al. reported connection frequencies consistent with our results. For the study of Huntgeburth et Petrides, there was a higher frequency of the “B pattern” (only RS-CS connection) from the left hemisphere and a lower frequency of the “E pattern” (more than one connection) on both sides. The study of Kim et al., on healthy individuals, had the same frequency differences as Huntgeburth et Petrides but with a lower frequency of the “A pattern” (no connection) from the right hemisphere. The origin of these differences have not been identified but could be caused by the manual ratings which are not strictly similar, the proportion of males/females not controlled for and the material used (MRI images versus *post mortem* studies). For the study of

Kim et al, the frequencies obtained in individuals with temporal lobe epilepsy (TLE) would require a large-scale study to be confirmed.

Regarding the association between sulcal connections and IHIs, an anatomical variation of the hippocampus, we were able to confirm our initial hypothesis that a link existed between the two. More specifically, RS-CS and CS-OTS connections on both sides are associated with a deeper collateral sulcus and more medial position of the hippocampus (**Table 5**). Most of the associations replicated in QTIM+QTAB (twelve out of sixteen and especially all those in the left hemisphere) (**Table 6**). To better understand this link, it will be necessary to consider more morphometric measurements of the sulci (surface, maximum depth, average depth, length, sulcal opening, etc.) in future studies. In a next step, we could also imagine targeting patients with IHI-related brain disorders (epilepsy, possibly autism, schizophrenia, etc.) to try to highlight a phenotypic association between these pathologies and some sulcal variations.

The heritability studies we performed have shown broad-sense heritability coefficients h^2 (Additive + Dominance) of 0.45 on the left and 0.30 on the right for the RS-CS connection as well as 0.30 on the left and 0.28 on the right for CS-OTS connection (**Table 8**). The sexual dimorphism for RS-CS (**Table 4**) as well as the negative tetrachoric correlation for opposite sex pairs (**Table 7**), could warrant to study whether the connection may be more heritable for one sex, and/or if different genetic loci contribute to the phenotype in each sex (sex-limitation models) but a larger number of twin pairs would be required to yield conclusive results. Reporting heritability is a first for these phenotypes, and opens the way to genome-wide association studies (GWAS), which could identify the genetic loci that cause these sulcal connections. Several studies have investigated the heritability of sulcal metrics (length, average depth, maximum depth, width, surface area), which vary greatly between metrics and brain regions (overall range 0-0.72) (Le Guen et al. 2018; Pizzagalli et al. 2020). Pizzagalli et al. meta-analyzed several twin studies (incl. QTIM) and showed that the collateral sulcus structure was under moderate genetic influence (e.g. $h^2=0.51$ for mean depth, $h^2=0.42$ sulcal width or

0.32 for surface area). In contrast, heritability of the anterior occipito-temporal sulcus appeared smaller (h^2 between 0.26-0.32) while it was around 0.19-0.24 for the rhinal sulcus structure. In addition, thickness and surface area of the neighboring gyri also display a moderate heritability (Strike et al. 2019). Future work should clarify which genetic variants cause the structural variation in the population, and whether sulci and gyri structure are influenced by variants that also contribute to the sulcal connections we reported here.

Sulcal connections tended to be largely symmetric as indicated by the large correlations between hemispheres that replicated in QTIM and QTAB (**Table 9 and 10**). Other research based on patterns has come to the same conclusion (Kim et al. 2008; Ovalioglu et al. 2018). We also found that, in general, there was a negative correlation between RS-CS and CS-OTS connections. Finally, we found large genetic correlations, particularly for the RS-CS and CS-OTS connections, which indicate that the co-occurrence of the sulcal connection is likely influenced by shared genetic factors (**Table 11**).

Our study has some limitations. First, we only considered three sulci and cannot generalise our findings throughout the brain. Our modular rating protocol allows to build on our results and progressively study other sulci. We will share our manual ratings for future reuse by interested researchers. Secondly, the number of twin pairs limited our investigation of the heritability, in particular to detect non-additive genetics or sex specific contributions. Thirdly, our use of a replication sample is a strength of the study and ensures replicated results are robust, however some sex dysmorphisms, co-occurrences, and association with IHIs did not replicate. The lack of replication is, to some extent, expected due to the winner's curse and a smaller replication sample, but it warrants future investigations in larger samples. Finally, the confidence interval of the frequencies for each connection does not systematically overlap between each database (IMAGEN versus QTIM versus QTAB). We can only hypothesise that this might be caused by a slight change in how the rater classified individuals after thousands

of classifications, unknown differences between the twin databases, or differences in image quality between studies.

Having demonstrated that the connections between the rhinal, collateral and occipito-temporal sulci have a stable frequency determined by genetic and environmental factors, our work calls to establish more precise classifications that include more sulci that would pave the way towards a global understanding of what create these anatomical variations. It remains unclear whether sulci connections could have a clinical significance. Using our classification principle and data, the development of an automatic sulci-connection classifier for future large-scale studies could accelerate this type of research.

5. Conclusion

In conclusion, our manual classifications over 3,400 individuals provide accurate evaluations of sulcal connection frequencies between the rhinal, collateral and occipito-temporal sulci. Our protocol may be extended to include connections with other sulci or the different sulcus patterns (side branches, number of segments, ...). In addition, we reported hemispheric asymmetries and sexual dimorphisms in sulci connections and showed that the connections exhibit broad sense heritability. Our study is the largest to date on sulcal connections, and suggests they are worth further investigation to clarify their possible association with behavior or disorders of the brain.

Source of funding and acknowledgements

The research leading to these results has received funding from the French government under management of Agence Nationale de la Recherche as part of the "Investissements d'avenir" program, reference ANR-19-P3IA-0001 (PRAIRIE 3IA Institute) and reference ANR-10-IAIHU-06 (Agence Nationale de la Recherche-10-IA Institut Hospitalo-Universitaire-6). BCD is supported by the NHMRC (CJ Martin Fellowship, APP1161356).

The Imagen study is supported by the following sources. This work received support from the following sources: the European Union-funded FP6 Integrated Project IMAGEN (Reinforcement-related behaviour in normal brain function and psychopathology) (LSHM-CT-2007-037286), the Horizon 2020 funded ERC Advanced Grant 'STRATIFY' (Brain network based stratification of reinforcement-related disorders) (695313), Human Brain Project (HBP SGA 2, 785907, and HBP SGA 3, 945539), the Medical Research Council Grant 'c-VEDA' (Consortium on Vulnerability to Externalizing Disorders and Addictions) (MR/N000390/1), the National Institute of Health (NIH) (R01DA049238, A decentralized macro and micro gene-by-environment interaction analysis of substance use behavior and its brain biomarkers), the National Institute for Health Research (NIHR) Biomedical Research Centre at South London and Maudsley NHS Foundation Trust and King's College London, the Bundesministerium für Bildung und Forschung (BMBF grants 01GS08152; 01EV0711; Forschungsnetz AERIAL 01EE1406A, 01EE1406B; Forschungsnetz IMAC-Mind 01GL1745B), the Deutsche Forschungsgemeinschaft (DFG grants SM 80/7-2, SFB 940, TRR 265, NE 1383/14-1), the Medical Research Foundation and Medical Research Council (grants MR/R00465X/1 and MR/S020306/1), the National Institutes of Health (NIH) funded ENIGMA (grants 5U54EB020403-05 and 1R56AG058854-01), NSFC grant 82150710554 and European Union funded project 'environMENTAL', grant no: 101057429. Further support was provided by grants from: - the ANR (ANR-12-SAMA-0004, AAPG2019 - GeBra), the Eranet Neuron

(AF12-NEUR0008-01 - WM2NA; and ANR-18-NEUR00002-01 - ADORe), the Fondation de France (00081242), the Fondation pour la Recherche Médicale (DPA20140629802), the Mission Interministérielle de Lutte-contre-les-Drogues-et-les- Conduites-Addictives (MILDECA), the Assistance-Publique-Hôpitaux-de-Paris and INSERM (interface grant), Paris Sud University IDEX 2012, the Fondation de l'Avenir (grant AP-RM-17-013), the Fédération pour la Recherche sur le Cerveau; the National Institutes of Health, Science Foundation Ireland (16/ERCD/3797), U.S.A. (Axon, Testosterone and Mental Health during Adolescence; RO1 MH085772-01A1) and by NIH Consortium grant U54 EB020403, supported by a cross-NIH alliance that funds Big Data to Knowledge Centres of Excellence.

The QTIM study was supported by the National Institute of Child Health and Human Development (R01 HD050735), and the National Health and Medical Research Council (NHMRC 486682, 1009064), Australia.

The QTAB study was funded by the National Health and Medical Research Council (NHMRC APP1078756), Australia. The QTAB study acknowledges the Queensland Twin Registry Study (<https://www.qimrberghofer.edu.au/study/queensland-twin-registry-study>) for generously sharing database information for recruitment. The QTAB study was further facilitated through access to Twins Research Australia, a national resource supported by a Centre of Research Excellence Grant (ID: 1078102) from the National Health and Medical Research Council.

We acknowledge access to the facilities and expertise of the CIBM Center for Biomedical Imaging, a Swiss research center of excellence founded and supported by Lausanne University Hospital (CHUV), University of Lausanne (UNIL), Ecole polytechnique fédérale de Lausanne (EPFL), University of Geneva (UNIGE) and Geneva University Hospitals (HUG).

Role of the funding source

The sponsors had no role in study design, data analysis or interpretation, writing or decision to submit the report for publication.

Data/Code Availability

Code used to process the data and perform the analyses will be available upon publication as <https://github.com/KevinDMR>.

The QTIM and QTAB dataset are in open access and available online at <https://openneuro.org/datasets/ds004169> and <https://openneuro.org/datasets/ds004146>.

The IMAGEN dataset is available to interested researchers upon application to the IMAGEN Executive Committee (ponscentre@charite.de, https://imagen-project.org/?page_id=547).

Authors contributions

Kevin de Matos had full access to all the data in the study and takes responsibility for the integrity of the data and the accuracy of the data analysis.

Study concepts and study design: KDM, BCD, OC, CC

Acquisition, analysis or interpretation of data interpretation: all authors

Manuscript drafting or manuscript revision for important intellectual content: all authors

Approval of final version of submitted manuscript: all authors

Literature research: KDM

Statistical analysis: KDM, BCD

Study supervision: BCD, OC, MBC, CC

Disclosure statement

Disclosure of interests related to the present article:

None to disclose.

Disclosure of interests unrelated to the present article:

OC reports having received consulting fees from AskBio and Therapanacea, having received fees for writing a lay audience short paper from Expression Santé, and that his laboratory has received grants (paid to the institution) from Qynapse. Members from his laboratory have co-supervised a PhD thesis with myBrainTechnologies and with Qynapse. OC's spouse is an employee of myBrainTechnologies. OC holds a patent registered at the International Bureau of the World Intellectual Property Organization (PCT/IB2016/0526993, Schiratti J-B, Allasonniere S, Colliot O, Durrleman S, A method for determining the temporal progression of a biological phenomenon and associated methods and devices).

Dr Banaschewski served in an advisory or consultancy role for eye level, Infectopharm, Lundbeck, Medice, Neurim Pharmaceuticals, Oberberg GmbH, Roche, and Takeda. He received conference support or speaker's fee by Janssen, Medice and Takeda. He received royalties from Hogrefe, Kohlhammer, CIP Medien, Oxford University Press. The present work is unrelated to the above grants and relationships. Dr Barker has received honoraria from General Electric Healthcare for teaching on scanner programming courses. Dr Poustka served in an advisory or consultancy role for Roche and Viforpharm and received speaker's fee by Shire. She received royalties from Hogrefe, Kohlhammer and Schattauer.

References

Auzias, G., M. Viellard, S. Takerkart, N. Villeneuve, F. Poinso, D. Da Fonséca, N. Girard, et C. Deruelle. 2014. « Atypical Sulcal Anatomy in Young Children with Autism Spectrum Disorder ». *NeuroImage: Clinical* 4: 593-603.
<https://doi.org/10.1016/j.nicl.2014.03.008>.

- Bajic, Dragan, Eva Kumlien, Peter Mattsson, Staffan Lundberg, Chen Wang, et Raili Raininko. 2009. « Incomplete Hippocampal Inversion—Is There a Relation to Epilepsy? » *European Radiology* 19 (10): 2544-50. <https://doi.org/10.1007/s00330-009-1438-y>.
- Bates, Timothy C., Hermine Maes, et Michael C. Neale. 2019. « Umx: Twin and Path-Based Structural Equation Modeling in R ». *Twin Research and Human Genetics* 22 (1): 27-41. <https://doi.org/10.1017/thg.2019.2>.
- Baulac, Michel, Nathalie De Grissac, Dominique Hasboun, Catherine Oppenheim, Claude Adam, Alexis Arzimanoglou, Franck Semah, Stephane Lehericy, Stephane Clémenceau, et Brigitte Berger. 1998. « Hippocampal Developmental Changes in Patients with Partial Epilepsy: Magnetic Resonance Imaging and Clinical Aspects: Hippocampal Developmental Changes and Epilepsy ». *Annals of Neurology* 44 (2): 223-33. <https://doi.org/10.1002/ana.410440213>.
- Bernasconi, N., D. Kinay, F. Andermann, S. Antel, et A. Bernasconi. 2005. « Analysis of Shape and Positioning of the Hippocampal Formation: An MRI Study in Patients with Partial Epilepsy and Healthy Controls ». *Brain* 128 (10): 2442-52. <https://doi.org/10.1093/brain/awh599>.
- Borrell, Víctor. 2018. « How Cells Fold the Cerebral Cortex ». *The Journal of Neuroscience* 38 (4): 776-83. <https://doi.org/10.1523/JNEUROSCI.1106-17.2017>.
- Cachia, Arnaud, Marie-Laure Paillère-Martinot, André Galinowski, Dominique Januel, Renaud de Beaurepaire, Frank Bellivier, Eric Artiges, et al. 2008. « Cortical Folding Abnormalities in Schizophrenia Patients with Resistant Auditory Hallucinations ». *NeuroImage* 39 (3): 927-35. <https://doi.org/10.1016/j.neuroimage.2007.08.049>.
- Chi, Je G, Elizabeth C Dooling, et Floyd H. Gilles. 1977. « Gyral Development of the Human Brain ». *Annals of Neurology* 1 (1): 86-93. <https://doi.org/10.1002/ana.410010109>.
- Cikla, Ulas, Guner Menekse, Arman Quraishi, Gabriel Neves, Abdullah Keles, Collin Liu, Shahriar M. Salamat, et Mustafa K. Baskaya. 2016. « The Sulci of the Inferior Surface of the Temporal Lobe: An Anatomical Study: Inferior Surface of the Temporal Lobe ». *Clinical Anatomy* 29 (7): 932-42. <https://doi.org/10.1002/ca.22767>.
- Cury, Claire, Roberto Toro, Fanny Cohen, Clara Fischer, Amel Mhaya, Jorge Samper-González, Dominique Hasboun, et al. 2015. « Incomplete Hippocampal Inversion: A Comprehensive MRI Study of Over 2000 Subjects ». *Frontiers in Neuroanatomy* 9 (décembre). <https://doi.org/10.3389/fnana.2015.00160>.
- Ecker, C., D. Andrews, F. Dell'Acqua, E. Daly, C. Murphy, M. Catani, M. Thiebaut de Schotten, et al. 2016. « Relationship Between Cortical Gyrfication, White Matter Connectivity, and Autism Spectrum Disorder ». *Cerebral Cortex* 26 (7): 3297-3309. <https://doi.org/10.1093/cercor/bhw098>.
- Gebre, Robel K., Matthew L. Senjem, Sheelakumari Raghavan, Christopher G. Schwarz, Jeffery L. Gunter, Ekaterina I. Hofrenning, Robert I. Reid, et al. 2023. « Cross-Scanner Harmonization Methods for Structural MRI May Need Further Work: A Comparison Study ». *NeuroImage* 269 (avril): 119912. <https://doi.org/10.1016/j.neuroimage.2023.119912>.
- Guadalupe, Tulio, Samuel R. Mathias, Theo G. M. vanErp, Christopher D. Whelan, Marcel P. Zwiers, Yoshinari Abe, Lucija Abramovic, et al. 2017. « Human Subcortical Brain Asymmetries in 15,847 People Worldwide Reveal Effects of Age and Sex ». *Brain Imaging and Behavior* 11 (5): 1497-1514. <https://doi.org/10.1007/s11682-016-9629-z>.
- Huntgeburth, Sonja C., et Michael Petrides. 2012. « Morphological Patterns of the Collateral Sulcus in the Human Brain: Morphology of the Collateral Sulcus ». *European Journal of Neuroscience* 35 (8): 1295-1311. <https://doi.org/10.1111/j.1460-9568.2012.08031.x>.
- Im, Kiho, Jong-Min Lee, Sang Won Seo, Sun Hyung Kim, Sun I. Kim, et Duk L. Na. 2008. « Sulcal Morphology Changes and Their Relationship with Cortical Thickness and

- Gyral White Matter Volume in Mild Cognitive Impairment and Alzheimer's Disease ». *NeuroImage* 43 (1): 103-13.
<https://doi.org/10.1016/j.neuroimage.2008.07.016>.
- Im, Kiho, Rudolph Pienaar, Jong-Min Lee, Joon-Kyung Seong, Yu Yong Choi, Kun Ho Lee, et P. Ellen Grant. 2011. « Quantitative Comparison and Analysis of Sulcal Patterns Using Sulcal Graph Matching: A Twin Study ». *NeuroImage* 57 (3): 1077-86.
<https://doi.org/10.1016/j.neuroimage.2011.04.062>.
- Im, Kiho, Nora Maria Raschle, Sara Ashley Smith, P. Ellen Grant, et Nadine Gaab. 2016. « Atypical Sulcal Pattern in Children with Developmental Dyslexia and At-Risk Kindergarteners ». *Cerebral Cortex* 26 (3): 1138-48.
<https://doi.org/10.1093/cercor/bhu305>.
- Jenkinson, Mark, Peter Bannister, Michael Brady, et Stephen Smith. 2002. « Improved Optimization for the Robust and Accurate Linear Registration and Motion Correction of Brain Images ». *NeuroImage* 17 (2): 825-41.
<https://doi.org/10.1006/nimg.2002.1132>.
- Jenkinson, Mark, et Stephen Smith. 2001. « A Global Optimisation Method for Robust Affine Registration of Brain Images ». *Medical Image Analysis* 5 (2): 143-56.
[https://doi.org/10.1016/S1361-8415\(01\)00036-6](https://doi.org/10.1016/S1361-8415(01)00036-6).
- Kim, H., N. Bernasconi, B. Bernhardt, O. Colliot, et A. Bernasconi. 2008. « Basal Temporal Sulcal Morphology in Healthy Controls and Patients with Temporal Lobe Epilepsy ». *Neurology* 70 (Issue 22, Part 2): 2159-65.
<https://doi.org/10.1212/01.wnl.0000313150.62832.79>.
- Kippenhan, J. S. 2005. « Genetic Contributions to Human Gyrfication: Sulcal Morphometry in Williams Syndrome ». *Journal of Neuroscience* 25 (34): 7840-46.
<https://doi.org/10.1523/JNEUROSCI.1722-05.2005>.
- Kong, Xiang-Zhen, Samuel R. Mathias, Tulio Guadalupe, ENIGMA Laterality Working Group, David C. Glahn, Barbara Franke, Fabrice Crivello, et al. 2018. « Mapping Cortical Brain Asymmetry in 17,141 Healthy Individuals Worldwide via the ENIGMA Consortium ». *Proceedings of the National Academy of Sciences* 115 (22).
<https://doi.org/10.1073/pnas.1718418115>.
- Kong, Xiang-Zhen, Merel C. Postema, Tulio Guadalupe, Carolien Kovel, Premika S. W. Boedhoe, Martine Hoogman, Samuel R. Mathias, et al. 2022. « Mapping Brain Asymmetry in Health and Disease through the ENIGMA Consortium ». *Human Brain Mapping* 43 (1): 167-81. <https://doi.org/10.1002/hbm.25033>.
- Kroenke, Christopher D., et Philip V. Bayly. 2018. « How Forces Fold the Cerebral Cortex ». *The Journal of Neuroscience* 38 (4): 767-75.
<https://doi.org/10.1523/JNEUROSCI.1105-17.2017>.
- Kruggel, Frithjof, et Ana Solodkin. 2020. « Heritability of Structural Patterning in the Human Cerebral Cortex ». *NeuroImage* 221 (novembre): 117169.
<https://doi.org/10.1016/j.neuroimage.2020.117169>.
- Le Guen, Yann, Guillaume Auzias, François Leroy, Marion Noulhiane, Ghislaine Dehaene-Lambertz, Edouard Duchesnay, Jean-François Mangin, Olivier Coulon, et Vincent Frouin. 2018. « Genetic Influence on the Sulcal Pits: On the Origin of the First Cortical Folds ». *Cerebral Cortex* 28 (6): 1922-33.
<https://doi.org/10.1093/cercor/bhx098>.
- Libero, Lauren E, Marie Schaer, Deana D Li, David G Amaral, et Christine Wu Nordahl. 2019. « A Longitudinal Study of Local Gyrfication Index in Young Boys With Autism Spectrum Disorder ». *Cerebral Cortex* 29 (6): 2575-87.
<https://doi.org/10.1093/cercor/bhy126>.
- Lohmann, G. 1999. « Sulcal Variability of Twins ». *Cerebral Cortex* 9 (7): 754-63.
<https://doi.org/10.1093/cercor/9.7.754>.
- Mohr, Alexander, Matthias Weisbrod, Peter Schellinger, et Michael Knauth. 2004. « The

- Similarity of Brain Morphology in Healthy Monozygotic Twins ». *Cognitive Brain Research* 20 (1): 106-10. <https://doi.org/10.1016/j.cogbrainres.2004.02.001>.
- Neale, Ben. 2014. « Liability Threshold Models ». In *Wiley StatsRef: Statistics Reference Online*, édité par N. Balakrishnan, Theodore Colton, Brian Everitt, Walter Piegorsch, Fabrizio Ruggeri, et Jozef L. Teugels, 1^{re} éd. Wiley. <https://doi.org/10.1002/9781118445112.stat06439>.
- Neale, Michael C, et Lon R Cardon. 2011. *Methodology for Genetic Studies of Twins and Families*. Dordrecht; London: Springer.
- Neale, Michael C., Michael D. Hunter, Joshua N. Pritikin, Mahsa Zahery, Timothy R. Brick, Robert M. Kirkpatrick, Ryne Estabrook, Timothy C. Bates, Hermine H. Maes, et Steven M. Boker. 2016. « OpenMx 2.0: Extended Structural Equation and Statistical Modeling ». *Psychometrika* 81 (2): 535-49. <https://doi.org/10.1007/s11336-014-9435-8>.
- Nordahl, C. W., D. Dierker, I. Mostafavi, C. M. Schumann, S. M. Rivera, D. G. Amaral, et D. C. Van Essen. 2007. « Cortical Folding Abnormalities in Autism Revealed by Surface-Based Morphometry ». *Journal of Neuroscience* 27 (43): 11725-35. <https://doi.org/10.1523/JNEUROSCI.0777-07.2007>.
- Novak, Klaus, Thomas Czech, Daniela Prayer, Wolfgang Dietrich, Wolfgang Serles, Stephan Lehr, et Christoph Baumgartner. 2002. « Individual variations in the sulcal anatomy of the basal temporal lobe and its relevance for epilepsy surgery: an anatomical study performed using magnetic resonance imaging ». *Journal of Neurosurgery* 96 (3): 464-73. <https://doi.org/10.3171/jns.2002.96.3.0464>.
- Ovalioglou, Aysegul Ozdemir, Talat Cem Ovalioglou, Gokhan Canaz, et Erhan Emel. 2018. « Morphologic Variations of the Collateral Sulcus on the Mediobasal Region of the Temporal Lobe: An Anatomical Study ». *World Neurosurgery* 118 (octobre): e212-16. <https://doi.org/10.1016/j.wneu.2018.06.156>.
- Penttilä, Jani, Marie-Laure Paillère-Martinot, Jean-Luc Martinot, Jean-François Mangin, Lisa Burke, Richard Corrigall, Sophia Frangou, et Arnaud Cachia. 2008. « Global and Temporal Cortical Folding in Patients With Early-Onset Schizophrenia ». *Journal of the American Academy of Child & Adolescent Psychiatry* 47 (10): 1125-32. <https://doi.org/10.1097/CHI.0b013e3181825aa7>.
- Penttilä, Jani, Marie-Laure Paillère-Martinot, Jean-Luc Martinot, Damien Ringuenet, Michèle Wessa, Josselin Houenou, Thierry Gallarda, et al. 2009. « Cortical Folding in Patients with Bipolar Disorder or Unipolar Depression ». *Journal of Psychiatry & Neuroscience: JPN* 34 (2): 127-35.
- Pereira, Joana Braga, Naroa Ibarretxe-Bilbao, Maria-Jose Marti, Yaroslau Compta, Carme Junqué, Nuria Bargallo, et Eduardo Tolosa. 2012. « Assessment of Cortical Degeneration in Patients with Parkinson's Disease by Voxel-Based Morphometry, Cortical Folding, and Cortical Thickness ». *Human Brain Mapping* 33 (11): 2521-34. <https://doi.org/10.1002/hbm.21378>.
- Pizzagalli, Fabrizio, Guillaume Auzias, Qifan Yang, Samuel R. Mathias, Joshua Faskowitz, Joshua D. Boyd, Armand Amini, et al. 2020. « The Reliability and Heritability of Cortical Folds and Their Genetic Correlations across Hemispheres ». *Communications Biology* 3 (1): 510. <https://doi.org/10.1038/s42003-020-01163-1>.
- Revelle, William. 2022. « psychTools: Tools to Accompany the 'psych; Package for Psychological Research ». <https://CRAN.R-project.org/package=psychTools>.
- Ritchie, Stuart J, Simon R Cox, Xueyi Shen, Michael V Lombardo, Lianne M Reus, Clara Alloza, Mathew A Harris, et al. 2018. « Sex Differences in the Adult Human Brain: Evidence from 5216 UK Biobank Participants ». *Cerebral Cortex* 28 (8): 2959-75. <https://doi.org/10.1093/cercor/bhy109>.
- Ronan, Lisa, et Paul C. Fletcher. 2015. « From Genes to Folds: A Review of Cortical Gyrfication Theory ». *Brain Structure and Function* 220 (5): 2475-83.

- <https://doi.org/10.1007/s00429-014-0961-z>.
- Routier, Alexandre, Ninon Burgos, Mauricio Díaz, Michael Bacci, Simona Bottani, Omar El-Rifai, Sabrina Fontanella, et al. 2021. « Clinica: An Open-Source Software Platform for Reproducible Clinical Neuroscience Studies ». *Frontiers in Neuroinformatics* 15 (août): 689675. <https://doi.org/10.3389/fninf.2021.689675>.
- Ruigrok, Amber N.V., Gholamreza Salimi-Khorshidi, Meng-Chuan Lai, Simon Baron-Cohen, Michael V. Lombardo, Roger J. Tait, et John Suckling. 2014. « A Meta-Analysis of Sex Differences in Human Brain Structure ». *Neuroscience & Biobehavioral Reviews* 39 (février): 34-50. <https://doi.org/10.1016/j.neubiorev.2013.12.004>.
- Strike, Lachlan T., Gabriella A.M. Blokland, Narelle K. Hansell, Nicholas G. Martin, Arthur W. Toga, Paul M. Thompson, Greig I. De Zubicaray, Katie L. McMahon, et Margaret J. Wright. 2022. « Queensland Twin IMaging (QTIM) ». *Openneuro*. <https://doi.org/10.18112/OPENNEURO.DS004169.V1.0.6>.
- Strike, Lachlan T., Narelle K. Hansell, Kai-Hsiang Chuang, Jessica L. Miller, Greig I. de Zubicaray, Paul M. Thompson, Katie L. McMahon, et Margaret J. Wright. 2022. « The Queensland Twin Adolescent Brain Project, a Longitudinal Study of Adolescent Brain Development ». Preprint. *Neuroscience*. <https://doi.org/10.1101/2022.05.19.492753>.
- Strike, Lachlan T., Narelle K. Hansell, Baptiste Couvy-Duchesne, Paul M. Thompson, Greig I. De Zubicaray, Katie L. McMahon, et Margaret J. Wright. 2019. « Genetic Complexity of Cortical Structure: Differences in Genetic and Environmental Factors Influencing Cortical Surface Area and Thickness ». *Cerebral Cortex* 29 (3): 952-62. <https://doi.org/10.1093/cercor/bhy002>.
- Strike, Lachlan T., Narelle K. Hansell, Jessica L. Miller, Kai-Hsiang Chuang, Paul M. Thompson, Greig I. De Zubicaray, Katie L. McMahon, et Margaret J. Wright. 2022. « Queensland Twin Adolescent Brain (QTAB) ». *Openneuro*. <https://doi.org/10.18112/OPENNEURO.DS004146.V1.0.3>.
- the IMAGEN consortium, G Schumann, E Loth, T Banaschewski, A Barbot, G Barker, C Büchel, et al. 2010. « The IMAGEN Study: Reinforcement-Related Behaviour in Normal Brain Function and Psychopathology ». *Molecular Psychiatry* 15 (12): 1128-39. <https://doi.org/10.1038/mp.2010.4>.
- Troiani, Vanessa, Will Snyder, Shane Kozick, Marisa A Patti, et Donielle Beiler. 2022. « Variability and Concordance of Sulcal Patterns in the Orbitofrontal Cortex: A Twin Study ». *Psychiatry Research: Neuroimaging* 324 (août): 111492. <https://doi.org/10.1016/j.psychresns.2022.111492>.
- Verweij, Karin J. H., Miriam A. Mosing, Brendan P. Zietsch, et Sarah E. Medland. 2012. « Estimating Heritability from Twin Studies ». In *Statistical Human Genetics*, éditée par Robert C. Elston, Jaya M. Satagopan, et Shuying Sun, 850:151-70. *Methods in Molecular Biology*. Totowa, NJ: Humana Press. https://doi.org/10.1007/978-1-61779-555-8_9.
- Wen, Junhao, Elina Thibeau-Sutre, Mauricio Diaz-Melo, Jorge Samper-González, Alexandre Routier, Simona Bottani, Didier Dormont, Stanley Durrleman, Ninon Burgos, et Olivier Colliot. 2020. « Convolutional Neural Networks for Classification of Alzheimer's Disease: Overview and Reproducible Evaluation ». *Medical Image Analysis* 63 (juillet): 101694. <https://doi.org/10.1016/j.media.2020.101694>.
- Yang, Guoyuan, Jelena Bozek, Meizhen Han, et Jia-Hong Gao. 2020. « Constructing and Evaluating a Cortical Surface Atlas and Analyzing Cortical Sex Differences in Young Chinese Adults ». *Human Brain Mapping* 41 (9): 2495-2513. <https://doi.org/10.1002/hbm.24960>.
- Yun, Hyuk Jin, Juan David Ruiz Perez, Patricia Sosa, J Alejandro Valdés, Neel Madan, Rie Kitano, Shizuko Akiyama, et al. 2021. « Regional Alterations in Cortical Sulcal Depth in Living Fetuses with Down Syndrome ». *Cerebral Cortex* 31 (2): 757-67.

<https://doi.org/10.1093/cercor/bhaa255>.

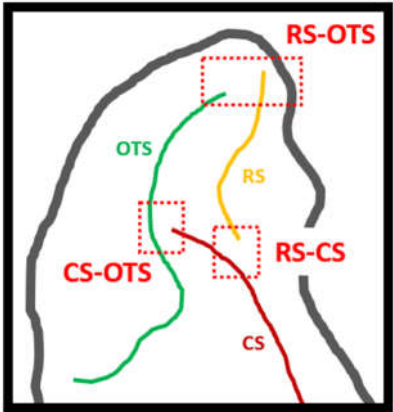
Zilles, Karl, Este Armstrong, Axel Schleicher, et Hans-Joachim Kretschmann. 1988. « The Human Pattern of Gyrification in the Cerebral Cortex ». *Anatomy and Embryology* 179 (2): 173-79. <https://doi.org/10.1007/BF00304699>.

Zubicaray, Greig I. de, Ming-Chang Chiang, Katie L. McMahon, David W. Shattuck, Arthur W. Toga, Nicholas G. Martin, Margaret J. Wright, et Paul M. Thompson. 2008. « Meeting the Challenges of Neuroimaging Genetics ». *Brain Imaging and Behavior* 2 (4): 258-63. <https://doi.org/10.1007/s11682-008-9029-0>.

Complement

Table S1. Pattern based classification

		CONNECTION-BASED		
		RS-CS	CS-OTS	RS-OTS
P A T T E R N - B A S E D	Type A	-	-	-
	Type B	X	-	-
	Type C	-	X	-
	Type D	-	-	X
	Type BC	X	X	-
	Type CD	-	X	X
	Type BD	X	-	X
	Type BCD	X	X	X
	Type E	Type BC + CD + BD + BCD		

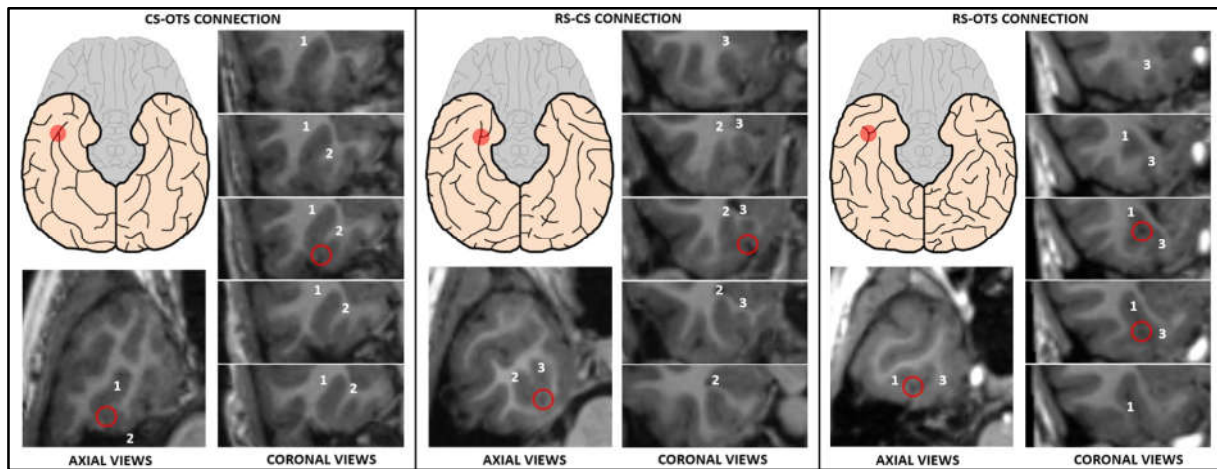


Each pattern (consideration of the 3 connections) is possible, from Type A to Type E. For example, type A represents no connection while type BC means that there are both RS-CS and CS-OTS connections but no RS-OTS connection. Type E was added because it corresponds to a type of classification used in other studies and allows comparison with our results. **X** = Connection; - = No connection; RS = Rhinal Sulcus; CS = Collateral Sulcus; OTS = Occipito-Temporal Sulcus

Figure S1. Databases visualization (MNI space)



Coronal view of IMAGEN (left), QTIM (center) and QTAB (right)

Figure S2. Connections assessment

1 = Occipito-temporal sulcus (OTS); 2 = Collateral sulcus (CS); 3 = Rhinal sulcus (RS);

Red circle = Sulcal connection

Left: we can see a connection between the occipito-temporal sulcus (1) and collateral sulcus (2) with the axial views (in schematic and MRI image) as well as the coronal views (taken at several levels before and after the connection).

Center: same principle but with a connection between the collateral sulcus (2) and the rhinal sulcus (3).

Right: same principle but with a connection between the occipito-temporal sulcus (1) and the rhinal sulcus (3).

Table S2. Frequency of connections with total number (Connection-based classification)

	IMAGEN	QTIM	QTAB	QTIM+QTAB
Left hemisphere				
RS-CS % (N)	40.3 (807)	37.2 (364)	34.6 (140)	36.4 (504)
Total / F / M	35.0 (360)	35.7 (216)	29.8 (59)	34.2 (275)
	45.8 (447)	39.7 (148)	39.1 (81)	39.5 (229)
CS-OTS % (N)	59.8 (1,198)	58.2 (570)	52.1 (211)	56.4 (781)
Total / F / M	64.3 (661)	61.6 (373)	53.0 (105)	59.6 (478)
	55.0 (537)	52.8 (197)	51.2 (106)	52.2 (303)
RS-OTS % (N)	10.6 (212)	6.7 (66)	9.1 (37)	7.4 (103)
Total / F / M	10.8 (111)	6.9 (42)	7.6 (15)	7.1 (57)
	10.3 (101)	6.4 (24)	10.6 (22)	7.9 (46)
Number of connections = 0	18.2 (364)	22.7 (222)	25.2 (102)	23.4 (324)
Total / F / M	18.4 (189)	20.8 (126)	27.8 (55)	22.5 (181)
% (N) Total / F / M	17.9 (175)	25.7 (96)	22.7 (47)	24.7 (143)
Number of connections = 1	57.3 (1,148)	52.7 (516)	58.0 (235)	54.3 (751)
Total / F / M	57.3 (589)	54.6 (331)	56.6 (112)	55.1 (443)
% (N) Total / F / M	57.3 (559)	49.6 (185)	59.4 (123)	53.1 (308)
Number of connections = 2	20.3 (407)	24.4 (239)	12.6 (51)	21.0 (290)
Total / F / M	20.1 (207)	24.3 (147)	13.1 (26)	21.5 (173)
% (N) Total / F / M	20.5 (200)	24.7 (92)	12.1 (25)	20.2 (117)
Number of connections = 3	4.2 (85)	0.2 (2)	4.2 (17)	1.4 (19)
Total / F / M	4.2 (43)	0.3 (2)	2.5 (5)	0.9 (7)
% (N) Total / F / M	4.3 (42)	0.0 (0)	5.8 (12)	2.1 (12)
Right hemisphere				
RS-CS % (N)	35.8 (718)	32.5 (318)	30.9 (125)	32.0 (443)
Total / F / M	27.9 (287)	28.7 (174)	23.2 (46)	27.4 (220)
	44.2 (431)	38.6 (144)	38.2 (79)	38.5 (223)
CS-OTS % (N)	31.1 (624)	31.0 (303)	24.0 (97)	28.9 (400)
Total / F / M	39.3 (404)	36.3 (220)	30.8 (61)	35.0 (281)
	22.5 (220)	22.3 (83)	17.4 (36)	20.5 (119)
RS-OTS % (N)	10.2 (205)	7.5 (73)	6.9 (28)	7.3 (101)
Total / F / M	9.9 (102)	8.1 (49)	6.1 (12)	7.6 (61)
	10.5 (103)	6.4 (24)	7.7 (16)	6.9 (40)
Number of connections = 0	36.2 (726)	41.1 (402)	45.2 (183)	42.3 (585)
Total / F / M	36.6 (376)	39.4 (239)	47.5 (94)	41.4 (333)
% (N) Total / F / M	35.9 (350)	43.7 (163)	43.0 (89)	43.4 (252)
Number of connections = 1	52.4 (1,051)	47.1 (461)	48.4 (196)	47.5 (657)
Total / F / M	51.9 (534)	48.2 (292)	46.0 (91)	47.6 (383)
% (N) Total / F / M	53.0 (517)	45.3 (169)	50.7 (105)	47.2 (274)
Number of connections = 2	9.0 (180)	11.7 (115)	5.9 (24)	10.0 (139)
Total / F / M	8.9 (92)	12.2 (74)	5.6 (11)	10.6 (85)
% (N) Total / F / M	9.0 (88)	11.0 (41)	6.3 (13)	9.3 (54)
Number of connections = 3	2.3 (47)	0.1 (1)	0.5 (2)	0.2 (3)
Total / F / M	2.5 (26)	0.2 (1)	1.0 (2)	0.4 (3)
% (N) Total / F / M	2.2 (21)	0.0 (0)	0.0 (0)	0.0 (0)

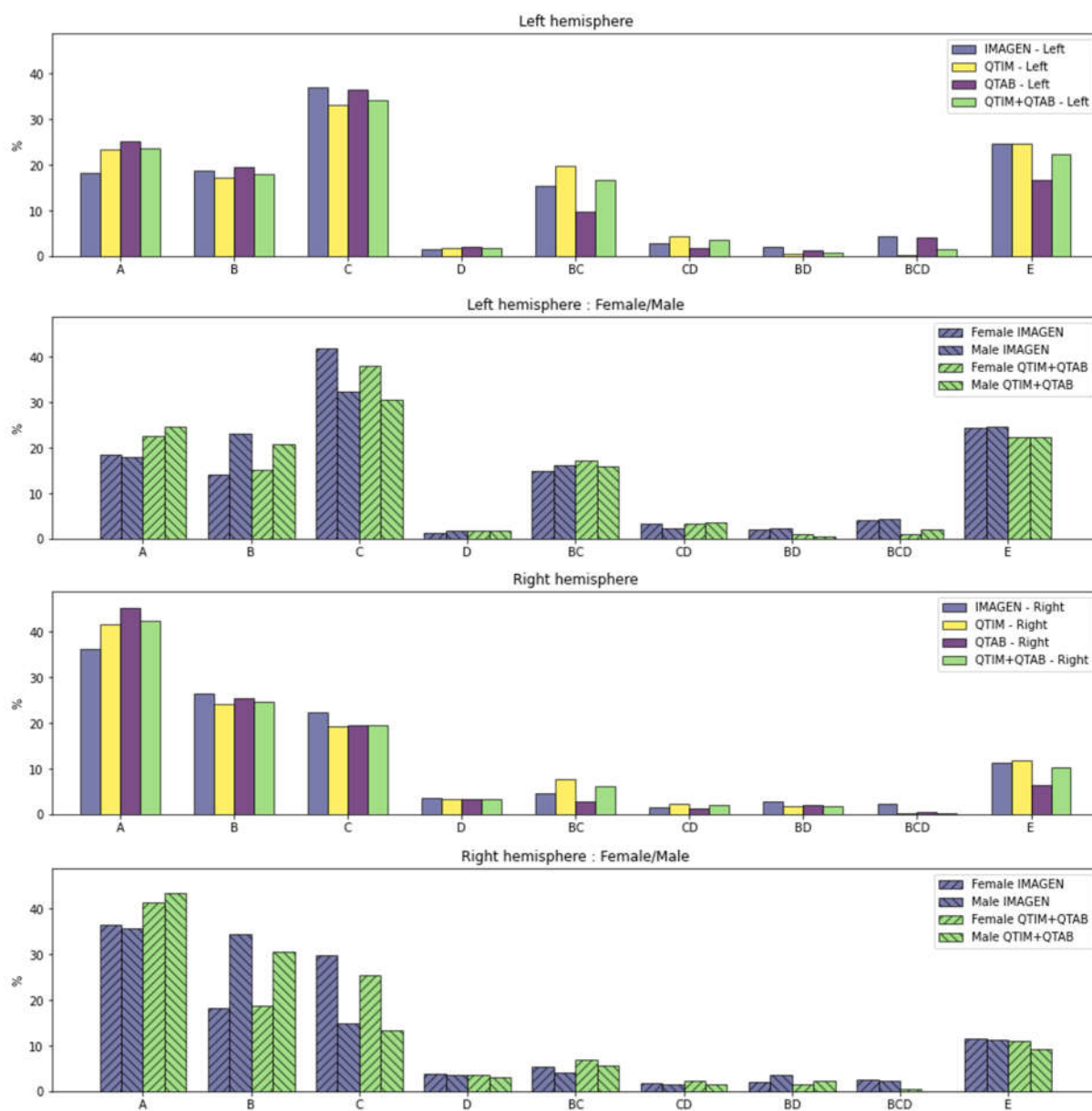
First line (bold) = Total frequency; Second line = Female frequency; Third line = Male frequency;
 RS = Rhinal Sulcus; CS = Collateral Sulcus; OTS = Occipito-Temporal Sulcus; F = Female; M = Male

Table S3. Frequency of pattern (Pattern-based classification)

	IMAGEN	QTIM	QTAB	QTIM+QTAB
Left hemisphere				
A % (N)	18.16 (364)	22.68 (222)	25.19 (102)	23.41 (324)
Total / F / M	18.39 (189) 17.93 (175)	20.79 (126) 25.74 (96)	27.78 (55) 22.71 (47)	22.51 (181) 24.66 (143)
B % (N)	18.51 (371)	16.75 (164)	19.51 (79)	17.56 (243)
Total / F / M	14.11 (145) 23.16 (226)	15.02 (91) 19.57 (73)	15.66 (31) 23.19 (48)	15.17 (122) 20.86 (121)
C % (N)	37.28 (747)	34.22 (335)	36.54 (148)	34.90 (483)
Total / F / M	41.93 (431) 32.38 (316)	37.79 (229) 28.42 (106)	38.89 (77) 34.30 (71)	38.06 (306) 30.52 (177)
D % (N)	1.50 (30)	1.74 (17)	1.98 (8)	1.81 (25)
Total / F / M	1.26 (13) 1.74 (17)	1.82 (11) 1.61 (6)	2.02 (4) 1.93 (4)	1.87 (15) 1.72 (10)
BC % (N)	15.47 (310)	19.61 (192)	9.63 (39)	16.69 (231)
Total / F / M	14.79 (152) 16.19 (158)	19.47 (118) 19.84 (74)	10.10 (20) 9.18 (19)	17.16 (138) 16.03 (93)
CD % (N)	2.79 (56)	4.19 (41)	1.73 (7)	3.47 (48)
Total / F / M	3.40 (35) 2.15 (21)	3.96 (24) 4.56 (17)	1.52 (3) 1.93 (4)	3.36 (27) 3.62 (21)
BD % (N)	2.05 (41)	0.61 (6)	1.23 (5)	0.79 (11)
Total / F / M	1.95 (20) 2.15 (21)	0.83 (5) 0.27 (1)	1.52 (3) 0.97 (2)	1.00 (8) 0.52 (3)
BCD % (N)	4.24 (85)	0.2 (2)	4.20 (17)	1.37 (19)
Total / F / M	4.18 (43) 4.30 (42)	0.33 (2) 0.00 (0)	2.53 (5) 5.80 (12)	0.87 (7) 2.07 (12)
E % (N)	24.55 (492)	24.61 (241)	16.79 (68)	22.32 (309)
Total / F / M	24.32 (250) 24.79 (242)	24.59 (149) 24.67 (92)	15.67 (31) 17.88 (37)	22.39 (180) 22.24 (129)
Right hemisphere				
A % (N)	36.23 (726)	41.06 (402)	45.19 (183)	42.27 (585)
Total / F / M	36.58 (376) 35.86 (350)	39.44 (239) 43.70 (163)	47.47 (94) 43.00 (89)	41.42 (333) 43.45 (252)
B % (N)	26.15 (524)	22.88 (224)	25.68 (104)	23.70 (328)
Total / F / M	18.19 (187) 34.53 (337)	18.81 (114) 29.49 (110)	18.18 (36) 32.85 (68)	18.66 (150) 30.69 (178)
C % (N)	22.60 (453)	20.74 (203)	19.51 (79)	20.38 (282)
Total / F / M	29.86 (307) 14.96 (146)	25.58 (155) 12.87 (48)	24.75 (49) 14.49 (30)	25.37 (204) 13.45 (78)
D % (N)	3.64 (73)	3.47 (34)	3.21 (13)	3.40 (47)
Total / F / M	3.79 (39) 3.48 (34)	3.80 (23) 2.95 (11)	3.03 (6) 3.38 (7)	3.61 (29) 3.10 (18)
BC % (N)	4.64 (93)	7.87 (77)	2.72 (11)	6.36 (88)
Total / F / M	5.25 (54) 4.00 (39)	8.09 (49) 7.51 (28)	3.54 (7) 1.93 (4)	6.97 (56) 5.52 (32)
CD % (N)	1.55 (31)	2.25 (22)	1.23 (5)	1.95 (27)
Total / F / M	1.65 (17) 1.43 (14)	2.48 (15) 1.88 (7)	1.52 (3) 0.97 (2)	2.24 (18) 1.55 (9)
BD % (N)	2.69 (54)	1.63 (16)	1.98 (8)	1.73 (24)
Total / F / M	1.95 (20) 3.48 (34)	1.65 (10) 1.61 (6)	0.51 (1) 3.38 (7)	1.37 (11) 2.24 (13)
BCD % (N)	2.35 (47)	0.1 (1)	0.49 (2)	0.22 (3)
Total / F / M	2.53 (26) 2.15 (21)	0.17 (1) 0.00 (0)	1.01 (2) 0.00 (0)	0.37 (3) 0.00 (0)
E % (N)	11.23 (225)	11.85 (116)	6.42 (26)	10.26 (142)
Total / F / M	11.38 (117) 11.06 (108)	12.39 (75) 11.00 (41)	6.58 (13) 6.28 (13)	10.95 (88) 9.31 (54)
Left vs Right pattern				
Same Pattern %	44.41	47.70	49.63	48.27
Total / F / M	46.30 42.42	49.50 44.77	52.53 46.86	50.25 45.52

For Pattern-based classification (from A to E), see Table S1. First line (bold) = Total frequency; Second line = Female frequency; Third line = Male frequency; F = Female; M = Male

Figure S3. Frequency of pattern (Pattern-based classification)



For Pattern-based classification (from A to E), see Table S1

Table S4. Comparison with other studies (Pattern-based classification)

Database	A	B	C	D	BC	CD	BD	BCD	E
Left hemisphere %									
IMAGEN (N=2,005)	18.16 [16.4 - 19.9]	18.51 [16.8 - 20.3]	37.28 [35.1 - 39.4]	1.50 [1.0 - 2.0]	15.47 [13.9 - 17.1]	2.79 [2.1 - 3.5]	2.05 [1.4 - 2.7]	4.24 [3.3 - 5.1]	24.55 [22.6 - 26.5]
QTIM (N=979)	22.68 [20.0 - 25.4]	16.75 [14.4 - 19.1]	34.22 [31.2 - 37.3]	1.74 [0.9 - 2.6]	19.61 [17.1 - 22.2]	4.19 [2.9 - 5.5]	0.61 [0.1 - 1.1]	0.20 [0.0 - 0.5]	24.62 [21.9 - 27.4]
QTAB (N=405)	25.19 [20.9 - 29.5]	19.51 [15.6 - 23.4]	36.54 [31.8 - 41.3]	1.98 [0.6 - 3.4]	9.63 [6.7 - 12.6]	1.73 [0.4 - 3.0]	1.23 [0.1 - 2.3]	4.20 [2.2 - 6.2]	16.79 [13.1 - 20.5]
Ovalioglu et al. 2018 (N=19) (healthy subjects)	28.57 [8.9 - 48.29] X	33.33 [12.8 - 53.9] X	28.57 [8.9 - 48.3] X	NA X	-	-	-	-	9.52 [0.0 - 22.3] X
Cikla et al. 2016 (N=35) (healthy subjects)	31.43 [15.7 - 47.1] X	17.14 [4.4 - 29.9] X	20.0 [6.5 - 33.5] X	NA X	-	-	-	-	31.43 [15.7 - 47.1] X
Huntgeburth et al. 2012 (N=40) (healthy subjects)	20.0 [7.4 - 32.7] X	40.0 [24.5 - 55.5] ↑	27.5 [13.4 - 41.6] X	10.0 [0.5 - 19.5] X	-	-	-	-	2.5 [0.0 - 7.4] ↓
Kim et al. 2008 (N=51) (healthy subjects)	15.69 [5.5 - 25.9] X	47.06 [33.1 - 61.0] ↑	31.37 [18.4 - 44.4] X	5.88 [0.0 - 12.5] X	-	-	-	-	NA ↓
Kim et al. 2008 (N=69) (TLE patients)	10.14 [2.9 - 17.4] ↓	76.81 [66.7 - 87.0] ↑	4.35 [0.0 - 9.3] ↓	8.7 [1.9 - 15.5] X	-	-	-	-	NA ↓
Right hemisphere %									
IMAGEN (N=2,005)	36.23 [34.1 - 38.4]	26.15 [24.2 - 28.1]	22.60 [20.7 - 24.5]	3.64 [2.8 - 4.5]	4.64 [3.7 - 5.6]	1.55 [1.0 - 2.1]	2.69 [2.0 - 3.4]	2.35 [1.7 - 3.0]	11.38 [10.0 - 13.0]
QTIM (N=979)	41.06 [37.9 - 44.2]	22.88 [20.2 - 25.6]	20.74 [18.1 - 23.3]	3.47 [2.3 - 4.6]	7.87 [6.1 - 9.6]	2.25 [1.3 - 3.2]	1.63 [0.8 - 2.4]	0.10 [0.0 - 0.3]	11.85 [9.8 - 13.9]
QTAB (N=405)	45.19 [40.2 - 50.1]	25.68 [21.3 - 30.0]	19.51 [15.6 - 23.4]	3.21 [1.5 - 5.0]	2.72 [1.1 - 4.3]	1.23 [0.1 - 2.3]	1.98 [0.6 - 3.4]	0.49 [0.0 - 1.2]	6.42 [4.0 - 8.9]
Ovalioglu et al. 2018 (N=19) (healthy subjects)	58.82 [35.0 - 82.7] X	11.76 [0.0 - 27.4] X	23.53 [3.0 - 44.1] X	NA X	-	-	-	-	5.88 [0.0 - 17.3] X
Cikla et al. 2016 (N=35) (healthy subjects)	45.71 [28.9 - 62.6] X	25.71 [10.9 - 40.5] X	17.14 [4.4 - 29.9] X	NA X	-	-	-	-	11.43 [0.7 - 22.2] X
Huntgeburth et al. 2012 (N=40) (healthy subjects)	37.5 [22.2 - 52.8] X	32.5 [17.7 - 47.3] X	22.5 [9.3 - 35.7] X	5.0 [0.0 - 11.9] X	-	-	-	-	2.5 [0.0 - 7.4] ↓
Kim et al. 2008 (N=51) (healthy subjects)	19.61 [8.5 - 30.7] ↓	41.18 [27.4 - 55.0] X	35.29 [21.9 - 48.7] X	3.92 [0.0 - 9.4] X	-	-	-	-	NA ↓
Kim et al. 2008 (N=69) (TLE patients)	11.59 [3.9 - 19.3] ↓	72.46 [61.7 - 83.2] ↑	4.35 [0.0 - 9.3] ↓	11.59 [3.9 - 19.3] X	-	-	-	-	NA ↓

For Pattern-based classification (from A to E), see Table S1. TLE = Temporal Lobe Epilepsy;
 First line = frequency in %; Second line = Confidence Interval (95%); Third line: X = in accordance with our CI
 (at least 2 of the 3 databases), ↑ (blue) = above our CI, ↓ (red) = below our CI